SKI Report 91:11

Radionuclide and Colloid Migration in Fractured Rock: Model Calculations

Peter Grindrod
David J. Worth

June 1990

ISSN 1104–1374
ISRN SKI-R-91/11-SE

SKI

Radionuclide and Colloid Migration in Fractured Rock: Model Calculations

Peter Grindrod - David J. Worth

SKI TR 91:11

INTERA/ECL
Environmental Sciences Department
Chiltern House
45 Station Road
Henley-on-Thames
Oxfordshire
RG9 1AT

June 1990

I2145-4
Version 1

Radionuclide and Colloid Migration in Fractured Rock: Model Calculations

Peter Grindrod

David J. Worth

June 1990

INTERA-ECL
Environmental Sciences Department
Chiltern House
45 Station Road
Henley-on-Thames
Oxfordshire
RG9 1AT
Tel: (0491) 410474
Tlx: 848776 ECL UK G
Fax: (0491) 576916

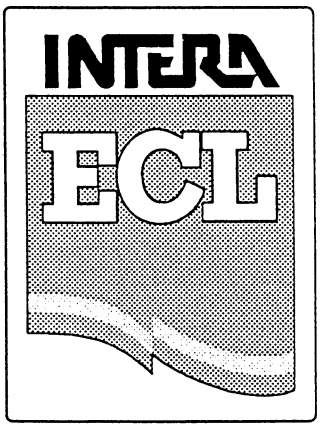

Summary

In this report, detailing the progress made in Phase II of the SKI radionuclide-colloid migration project, the model specified in Phase I is further refined and calculations of radionuclide dispersal and transport are made assuming a background level of colloids, free and immobile, present in the fractured rock.

Model data requirements include dispersion rates, flow rates, and sorption rates for colloids in fractured rock. Accordingly, such data is derived, and its dependence upon colloid size, composition, fracture size, and microscopic surface forces analyzed.

In the subsequent radionuclide-colloid analysis, radionuclides bound to colloids disperse with such characteristics, and the enhancement or retardation of radionuclide migration due to colloidal sorption is assessed.

The colloid migration analysis in this report is based upon theoretical considerations and does not rely on macroscopic, empirically defined constants. We discuss possible validation of the methodology, and use the results to make predictions for individual colloid penetration. We obtain the quantitative behaviour of the transport parameters, taking suitable values for the fracture width, groundwater flow rate, and a range of forces due to surface charge. The numerical algorithm used has been verified against analytic results in the special case where surface charges are negligible.

The calculated breakthrough curves for radionuclides illustrate the effects of colloids. The radionuclides are present within the fracture either in solution, bound to free colloids, or bound to immobile colloid material. Radionuclides may also diffuse into the pore space and become sorbed to the porous rock surfaces.

We present a unified theoretical approach spanning considerations of dispersal and surface forces on the scale of individual colloids $O(10^{-8}\mathrm{m})$, up to the breakthrough behaviour over length scales $O(10^{3}\mathrm{m})$. One major achievement of this work is to address the gap between standard continuum migration models, where best-fit parameters are often determined from the available experimental and field data, and the considerations of colloid science, where natural and synthetic colloids and complexes are subject to microscopic analysis.

Contents

1 Introduction

The precise role of colloids in the transport and dispersal of radionuclides through fractured and porous rock is, to date, poorly understood. Although some laboratory and field data regarding colloid and groundwater chemistry is available, there have been few attempts to incorporate such information into a dynamic colloid migration model.

Radionuclides present in groundwater sorb strongly on to rock surfaces. Not all such surfaces are immobile though, and it is well known that radionuclides may become sorbed to colloidal particles present within the groundwater. Once sorbed to colloids, their transportation becomes radically altered. Amongst other properties, the fact that colloids are advected by the fluid flow at a faster mean rate than dissolved nuclides has been well-documented. Thus, if a significant proportion of the available radionuclides become colloid-bound, the non-colloid models may underestimate the transit speeds (possibly by as much as $30 - 40\%$).

In Phase I of the SKI radionuclide-colloid modelling project a number of conceptual factors were identified, reviewed and formulated as a mathematical nuclide-colloid transport model [10]. In Phase II this work was utilised as the basis for both modelling and calculations of colloid migration and the subsequent effect upon the transport and dispersal of radionuclides in fractured rock. This report documents the results from Phase II.

In addition to the model calculations, it was necessary to develop a mathematical technique capable of reducing the microscopic mathematical models of the processes affecting colloids in water-filled fractures, to the macroscopic parameters defining colloid dynamics over much larger scales. This work provides a firm theoretical basis for the subsequent model calculations, and allows the calculation of dynamic parameters that are otherwise unavailable. We must pass from the consideration of surface forces and dispersal on the scale of individual colloids $O(10^{-8})$m to that of the radionuclide dispersal models in fractures, where nuclides must travel over distances $O(10^{3})$m. Thus our analysis incorporates effects valid on spatial scales differing by eleven orders of magnitude. The mathematical technique, based upon an asymptotic comparison of spectra, is derived in the appendix of this report.

There is a large literature concerning the chemistry of colloids and complexes. This involves the analysis of naturally occurring colloids, groundwater chemistry, and batch experiments on radionuclide-colloid sorption. However, much of this work, including the consideration of different kinds

of s e forces, has largely ignored the dynamical aspects of colloids.

On the other hand, a number of advection-dispersion-sorption equations utilized in previous migration models, reviewed in [10] (a more recent example being [11]), make no attempt to tie the parameters controlling the dispersal of colloids, in fractured or porous media, to the underlying colloid science. They are merely numbers to be determined.

One of the central aims of the work presented here is to bridge the void between these opposing viewpoints by developing the underlying principles, formulated in [10], into a colloid migration model acceptable on large spacial scales, in a coordinated fashion. The resulting calculations of radionuclide migration and dispersal in the presence of colloids compare directly to the no-colloid case, and allow us to consider the effects of fracture aperture, flow rates, colloid size, colloid density, and surface forces upon the subsequent enhancement or retardation of radionuclides .

In section 2 we discuss the colloid migration models and derive parameters governing colloid dispersal from a consideration of the underlying physical and chemical processes. We have taken the analysis in [10] much further in order to discuss quantitatively the behaviour of colloids in a single fracture. The mathematical technique is more sophisticated than that of [10] and is expounded in detail within the appendix.

In sections 3 and 4 we utilize the results from the colloid dispersal calculations of section 2 in order to assess the effect upon radionuclide migration within the fractured rock. In particular we model the dispersal of radionuclides assuming background populations of colloids, both free and immobile, to which they may become sorbed. Breakthrough curves are calculated allowing unknown partition coefficients to vary over four orders of magnitude independently.

In section 5 we discuss some extensions of the basic model scenario.

Finally in section 6 we make concluding remarks and observations indicating the major achievements of Phase II of the SKI Radionuclide Colloid modelling initiative.

2 Colloid migration and dispersal

In this section, we shall consider colloid dispersal in a single, idealised fracture. As discussed in [10], this must present the colloids with their best opportunity to migrate over *long* distances, at average flow rates 20-30% in excess of that of any solutes present. Since the real flow paths are irregular and tortuous, this would both perturb the assumed flow rate, and increase the rock surface area available for colloid adsorption.

Radionuclides are transported both in solution and adsorbed to colloids. In order to analyse radionuclide-colloid fracture transport models in section 3 (including matrix diffusion and retardation of the solute in the surrounding rock), robust quantitative values for colloid transport parameters, as compared to the solute, are required as **input data**.

The idealised fracture is also suggestive of dynamic colloid migration experiments that could be carried out utilising capillary tubes, of suitable material in order to measure colloid dispersal and validate the modelling approach.

In [10] there is a brief review of colloid migration modelling along with the conceptual and mathematical specification of the microscopic models used as the starting point below.

The aim of the current section is to make the calculation of the macroscopic flow parameters, valid on length scales many orders of magnitude larger than that associated with individual colloids and surface forces, for colloids explicit, emphasising their dependence upon the chemical and physical data available from laboratory and field studies. We obtain a colloid migration model, using such parameters, which may be solved to estimate colloid migration and dispersal within the fracture.

In [10], a number of models are discussed for nuclide-colloid migration in a single rock fracture. Consideration is given to the mathematical form of surface forces acting on the colloids, as well as the diffusive and advective processes present.

Rather than deal with full three dimensional fractures, it is more relevant, and more tractable, to consider the dispersal of colloids in a single direction - the direction of the groundwater flow. Accordingly, in the Appendix of this report, a method is derived for reducing the full three dimensional models to one dimensional axial flow models. This method may properly be thought of as a generalisation of the approach used by standard Taylor dispersion theory for solutes in impermeable pipes or fractures. The novel element is that, in the colloid model, we must allow for the cross-fracture

advection due to surface forces and for the adsorption of colloids to the fracture faces. Thus we must calculate an axial dispersivity (due to both molecular diffusion and hydrodynamic dispersion), an average advection rate (due to groundwater flow), and a sorption rate for colloids in the fracture. All of these terms are size dependent. We consider colloids having radii in the range (10-1000 nm).

The plan of this section is as follows. We outline a full fracture transport model for a population of spherical colloids of uniform radius, a. Owing to the linearity of the problem, the behaviour of colloids of differing sizes may be superimposed. In section 2.2, we discuss a one dimensional model for colloid transport in the direction of the advective groundwater flow. The macroscopic flow parameters are derived in a number of cases using the asymptotic comparison method developed in the appendix to this report. In section 2.3, we discuss some solutions of the models derived in section 2.2. Specifically, we consider the evolution of colloids released into an infinite fracture as well as the time dependent and steady state distributions when colloids are supplied at a given concentration at a fracture inlet.

The sorption of radionuclides to colloids is reversible so that even though individual colloids are not transported over relatively large distances, the nuclides may exchange (repeatedly) from the solute to colloid-bound states, taking advantage of the increased colloid flow rates.

2.1 Colloid Migration in a Single Fracture

We consider colloids having hydrodynamic radii, a, in the range 10-1000 nm. We shall assume that the hydrodynamic radius is equal to the average physical radius of the colloids, though the generalisation is straightforward. Moreover, the models discussed in this section are linear with respect to the colloid density functions, so the distributions of colloids of different sizes may be superimposed. Hence there is no loss of generality in assuming a population of colloids having uniform radius a, and allowing this to vary.

Following [10], we consider a uniform planar fracture of half width L (in metres), see figure 1.

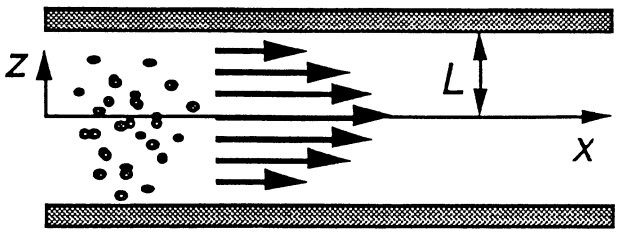

Figure 1: The fracture.

We assume that the migration problem is symmetrical about the centre plane ($z = 0$). The equations derived in [10] governing the dispersal of spherical colloids, having radius a(m), in the absence of sources, are given by

$$\begin{aligned} c_t &= D(c_{xx} + c_{zz}) - (cv(z))_z - u(z)c_x \qquad (1)\\ &\qquad \text{for } 0 < z < L - a, \quad t > 0;\\ c_z = 0 \quad &\text{at} \quad z = 0,\\ c = 0 \quad &\text{at} \quad z = L - a, \end{aligned}$$

where $c(x, z, t)$ denotes the density function for colloids in the fracture. Colloids at $z = L - a$ are in contact with the rock face and are assumed to be adsorbed there (hence the boundary condition).

The terms in (1) are defined as follows.

D is the diffusivity of colloids with radius a, in groundwater. It is given by the Stokes-Einstein relation

$$D = \frac{\tilde{D}}{a} \qquad (\mathrm{m}^2/\mathrm{yr}). \qquad (2)$$

$\tilde{D}$ is a constant given by

$$\tilde{D} = \frac{k_b T}{6\pi\mu} \qquad (\mathrm{m}^3/\mathrm{yr}),$$

where k_b is the Boltzmann constant, T is the absolute temperature, and μ is the viscosity of groundwater. Typical values are given in table 1 below.

The groundwater flow is assumed to be so slow that Poiseuille approximation is valid. We have

$$u(z) = \frac{3}{2}u_0\Big(1 - \frac{z^2}{L^2}\Big) \qquad (\mathrm{m/yr}) \qquad (3)$$

where the constant u_0 denotes the cross-fracture average velocity.

L	10^{-4} m
a	$10^{-8} - 10^{-6}$ m
k_b	1.38×10^{-23} J/K
T	270-280 K
μ	3.8×10^{-11} Nyr/m^2
	5.4×10^{-12} m^3/yr
u_0	$10 - 50$ m/yr
χ	$O(10^8)$ m^{-1}
η	$10^{-19} - 10^{-21}$ J

Table 1: Parameter values.

Colloids are subject to surface forces acting across the fracture. Free colloids are also subject to drag forces opposing their motion relative to the groundwater. As in [10], we shall write

$$v(z) = \frac{F(z,a)}{6\pi\mu a}, \tag{4}$$

where $v(z)$ denotes the cross-fracture component of the velocity of colloids, of radius a, as a function of their cross-fracture location, z. $F(z,a)$ is the surface force, acting on colloids in the z-direction, due to the presence of the rock surfaces.

Following [10], $F(z,a)$ is the sum of separate terms. The force on a colloid due to the presence of electric double layers (surface charges) is of the form

$$-\frac{8y_c y_r a m k_b T \pi}{\chi} \exp(-\chi(L-a)) \sinh \chi z, \tag{5}$$

where y_c and y_r are dimensionless potentials of the colloidal and rock surface (assumed equal for both rock faces); χ is the Debye-Huckel parameter (see table 1); m is the number of ions per unit volume in the groundwater (m^{-3}) (see [9] for a fuller description).

If $y_c y_r > 0$, as for example when the colloids and the rock are of similar composition, then this force is repulsive, causing the colloids to stay more centre stream.

The van der Waals force, due to the interaction of molecules on the colloid and rock surfaces, is attractive but acts over short distances. It is given here by

$$\frac{2}{3} \frac{a(L-a)z\eta}{((L-a)^2 - z^2)},$$

where η is the Hamaker constant, depending upon the composition of the colloid and rock surfaces (see table 1).

Other long or short range forces may be considered within our present approach. We merely require their functional form together with associated parameter values. In view of the ongoing debate on surface forces, it seems wise to allow for alternative theories to be included in any model for colloid dispersal. For example DLVO theory, based upon surface charges and molecular interactions, has been recently questioned [8].

In this report, we shall concentrate on the effect of surface charges held on the colloids and the rock faces. From (4) and (5), we obtain

$$v(z) = -\frac{8y_c y_r m k_b T}{6\mu\chi} \exp(-\chi(L-a)) \sinh \chi z \quad \text{(m/yr)}. \tag{6}$$

In [10], we use a van der Waals type term, but this is likely to be of importance only where the colloids are extremely close to the walls. Thus we shall assume that the sorption process itself is initiated by large attractive van der Waals forces between the colloids and the rock faces, whilst the forces due to surface charges, giving rise to (6), are dominant away from the fracture (see [9]) also. Further centre stream diffusion is the dominant dispersal phenomena.

2.2 One Dimensional Transport Models

Despite the complexity of its terms, (1) represents a linear diffusion-advection-sorption process albeit in a two dimensional spatial domain ((x, z)-space).

In the appendix we show how problems in the form of (1) may be reduced to one dimensional transport models via an asymptotic spectral comparison method. Employing this technique here, we obtain a model of the form

$$c_t = D^* c_{xx} - u^* c_x - s^* c, \tag{7}$$

where the parameters D^* (m^2/yr), u^* (m/yr) and s^* (1/yr) depend upon L, a, D, $u(z)$ and $v(z)$. Here, c is used to denote the distribution of colloids per unit fracture length (colloids per m, whereas $c(x, z, t)$ in (1) is colloids per m^2).

The sorption rate, s^*, the average velocity, u^*, and the effective diffusion term, D^*, are calculated by seeking to solve (1) in a certain asymptotic limit. This is a generalisation of Taylor dispersion theory. Here, we utilize the $c = 0$ boundary condition at $z = L - a$, as well as the cross-fracture advection term, $v(z)$: both effects are absent in classical Taylor dispersion

[16]. The precise details are not relevant here, sa[illegible]r the fact that the method is valid for solutions dominated by small w[illegible]e numbers in the x-direction (for example, for smooth distributions or large time). Note also that the sorption process (modelled in the boundary condition imposed on the full model) appears as a dynamic loss rate in (7). The relevant mathematical theory is developed in the appendix.

The full calculation of D^*, u^* and s^* is analytically intractable unless $v \equiv 0$. However, their numerical computation is straightforward and we have an algorithm based on the method in the appendix.

In the special case where $v \equiv 0$, we obtain s^*, u^* and D^* analytically. We have

$$\begin{aligned} s^* &= \frac{D\pi^2}{4(L-a)^2} \\ u^* &= \frac{3}{2}u_0\left\{1 - 2\left(\frac{1}{6} - \frac{1}{\pi^2}\right)\frac{(L-a)^2}{L^2}\right\} \\ D^* &= D + \frac{(L-a)^6}{L^4}\frac{u_0^2}{D}\frac{0.026303995}{\pi^2} \end{aligned}$$

(where $D = \tilde{D}/a$).

Thus for $v \equiv 0$, we have verified our numerical code directly, see figure 2 where s^*, u^*, D^* are shown as functions of a. The parameter values used are as in table 1. We also graph $x^* = u^*/s^*$, which is the mean distance travelled by individual colloids in the fracture.

Note that in all numerical calculations we have used millimetres, rather than metres, in order to obtain more manageable orders of magnitude.

To include the effects of surface forces ($v \not\equiv 0$), we analyse the same problem, taking

$$v(z) = -v_0 \sinh(\chi z)\exp(-(L-a)\chi),$$

as in (6).

Here v_0 and χ are constants. Although v depends upon the chemical properties of the rock faces and the colloids, we may assess the sensitivity of results to $v(z)$ by allowing v_0 to vary over a number of orders of magnitude. When $v_0 > 0$, the colloids are repelled from the rock faces, and consequently s^* should be decreased and u^* increased. We may also expect that D^* decreases with respect to v_0 since colloids stay more centre stream which lessens the effect of the hydrodynamic flow profile. When $v_0 < 0$, colloids are attracted towards the adsorbing rock faces, and hence

s^* should be relatively large while u^* is smaller. Thus for fixed a, x^* ought to be increasing with the parameter v_0. In figure 3 we show values for D^*, s^*, u^* and x^* as functions of a, taking v_0=0, 10^3, $10^{7/2}$, 10^4 mm/yr. For simplicity, we have taken $\chi = 1$. This also exaggerates the effect of surface charges.

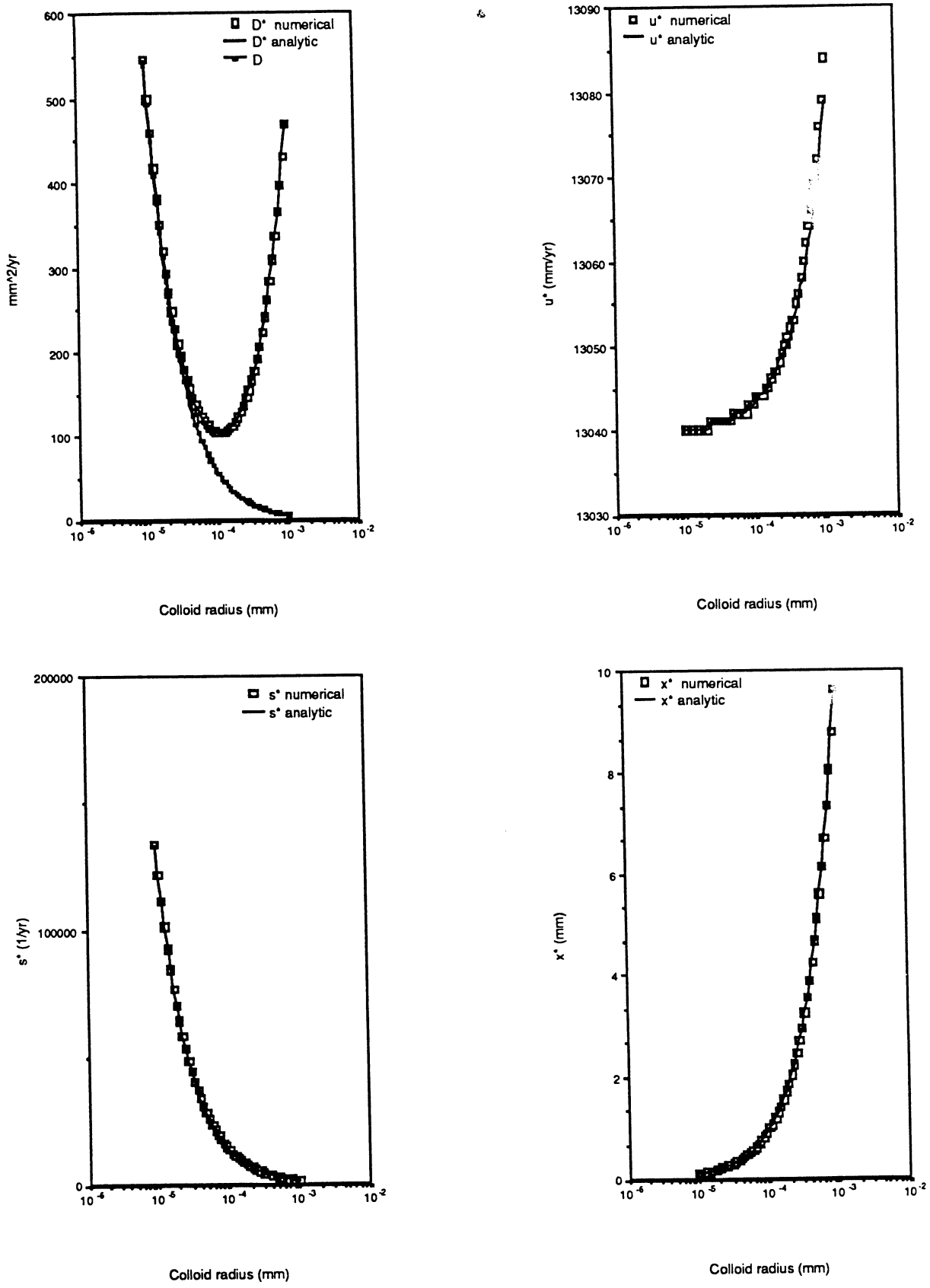

Figure 2: Analytical verification of the numerical method for generating macroscopic flow parameters.

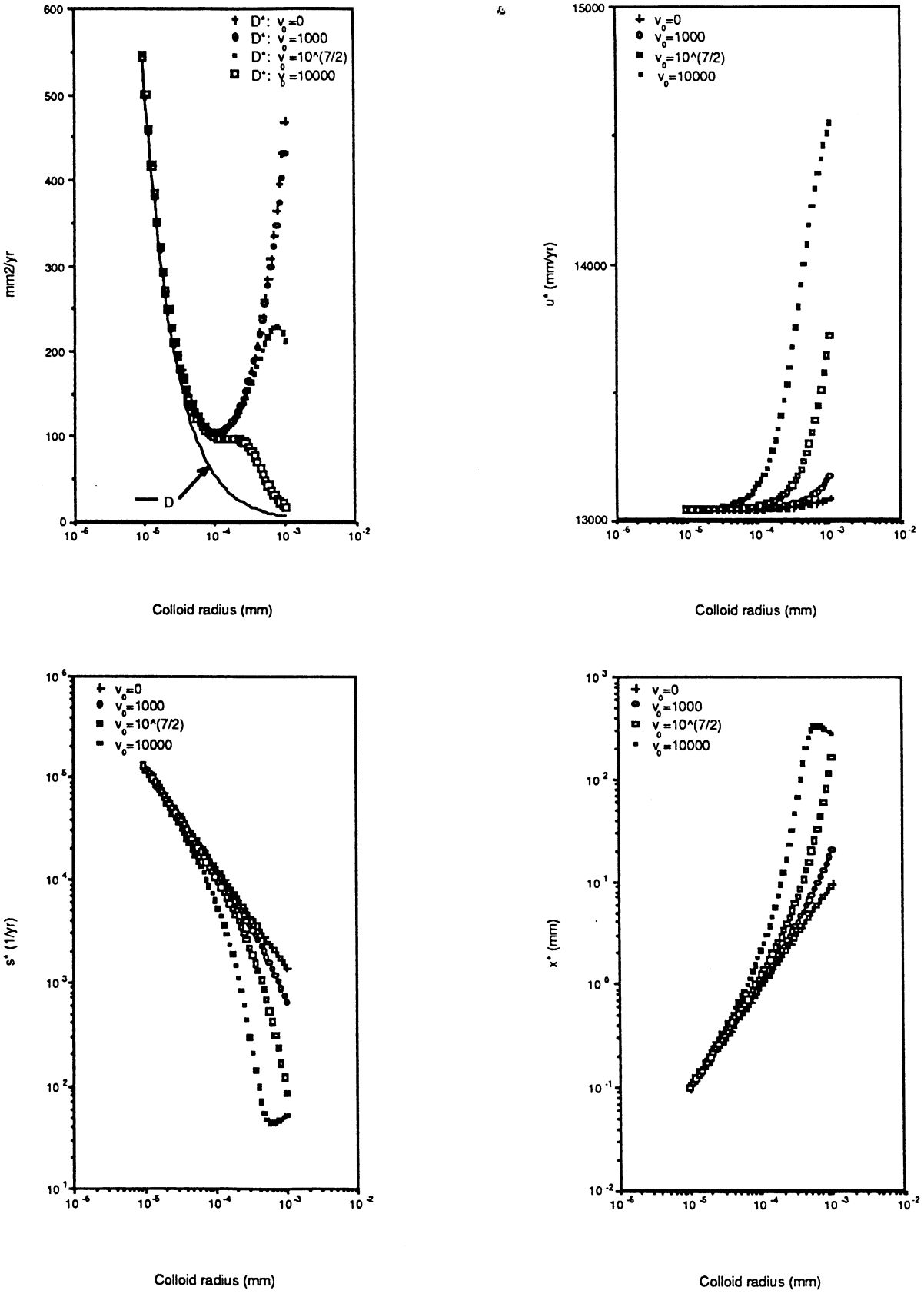

Figure 3: Graphs of numerical results showing the effect of increasing the surface charges.

We make the following remarks concerning the results depicted in figure 3:

- The values of D^* differ significantly over the range 30-1000nm. For smaller colloids, we have $D^* \approx D$.
- As v_0 is increased, the effect of hydrodynamic dispersion becomes less important, although D^* remains an order of magnitude greater than D for colloids $O(100\,\text{nm})$.
- The effects of size and surface charge upon u^* and s^* were as anticipated. In particular, the mean distance of individual colloid migration increases with v_0, especially for the larger colloids.
- x^* is of the order of 1-100 cm. Clearly these results depend delicately upon surface charge. There is also an obvious dependency upon a, u_0 and L. If $v_0 = 0$ and $0 < a \ll L$, we obtain

  $$x^* = \frac{aL^2u_0}{D\pi^2}(1 + \frac{3}{\pi^2}),$$

  illustrating the sensitivity of x^* to our particular choice of parameter values.

It remains to specify the true value for v_0 (given a certain class of colloids) and χ given a certain groundwater chemistry. In table 1, we have given a value for χ approximate to those given in [9].

Our calculations have a further utility, since the scaling of D^* and u^* with respect to u_0 can be shown to obey simple relationships (s^* is independent of u^*). If $u_0 \neq 10000\,\text{mm/yr}$, as it was for the calculations in figure 3, then the new values for D^* and u^* are given by

$$D + (D^*_G - D)\frac{u_0^2}{10^8} \qquad \text{mm}^2/\text{yr},$$

$$u^*_G \cdot \frac{u_0}{10^4} \qquad \text{mm/yr}$$

respectively, where D^*_G (mm^2/yr) and u^*_G (mm/yr) are read from the graphs previously calculated. (Note that when $v_0 \equiv 0$, our analytical expressions obey this scaling).

2.3 Analytical Solutions

Consider (5) modelling a fracture of infinite extent in the axial direction of water flow. A population of M colloids supplied at $x = 0$ at $t = 0$ yields the solution

$$c = Me^{-s^*t}\left(\frac{e^{-(x-u^*t)^2/4tD^*}}{\sqrt{4\pi tD^*}}\right).$$

In particular, the mean position of the colloids is given by

$$x = u^*t,$$

while the variance is given by

$$\sigma^2 = 2Dt.$$

The population mass is simply

$$Me^{-s^*t}.$$

A key question is what fraction, H, of colloids penetrate to a distance greater than some X, fixed, before becoming sorbed to the rock face?

This is equal to the fraction of colloids sorbed to the rock at $x > X$ over all time. That is a fraction, $H(X)$, of colloids given by

$$\begin{aligned} H &= \int_0^\infty \int_X^\infty s^* c(x,t)\, dX\, dt \\ &= \int_0^\infty \frac{s^*}{2} e^{-s^*t} \mathrm{erfc}\left(\frac{X - u^*t}{\sqrt{4tD^*}}\right) dt \\ &= \frac{s^*}{2\sqrt{\mu}(\sqrt{\mu} - \frac{u^*}{\sqrt{4D^*}})} \exp\left(-\frac{X}{\sqrt{D^*}}\left(\sqrt{\mu} - \frac{u^*}{\sqrt{4D}}\right)\right) \end{aligned}$$

where

$$\mu = s^* + \frac{u^{*2}}{4D^*}.$$

Choosing D^* etc given in tables 2 and 3, we have $H = H(X)$ as shown in figure 4.

a (mm)	10^{-5}	10^{-4}	10^{-3}
D^* (mm^2/yr)	545	103	470
s^* (1/yr)	133000	13400	1360
u^* (mm/yr)	13000	13000	13100

Table 2: Typical parameter values for $u_0 = 10000\,\text{mm/yr}$ (using $v(z) \equiv 0$).

a (mm)	10^{-5}	10^{-4}	10^{-3}
D^* (mm^2/yr)	663	1280	11600
s^* (1/yr)	133000	13400	1360
u^* (mm/yr)	65200	65200	65400

Table 3: Typical parameter values for $u_0 = 50000\,\text{mm/yr}$ (using $v(z) \equiv 0$).

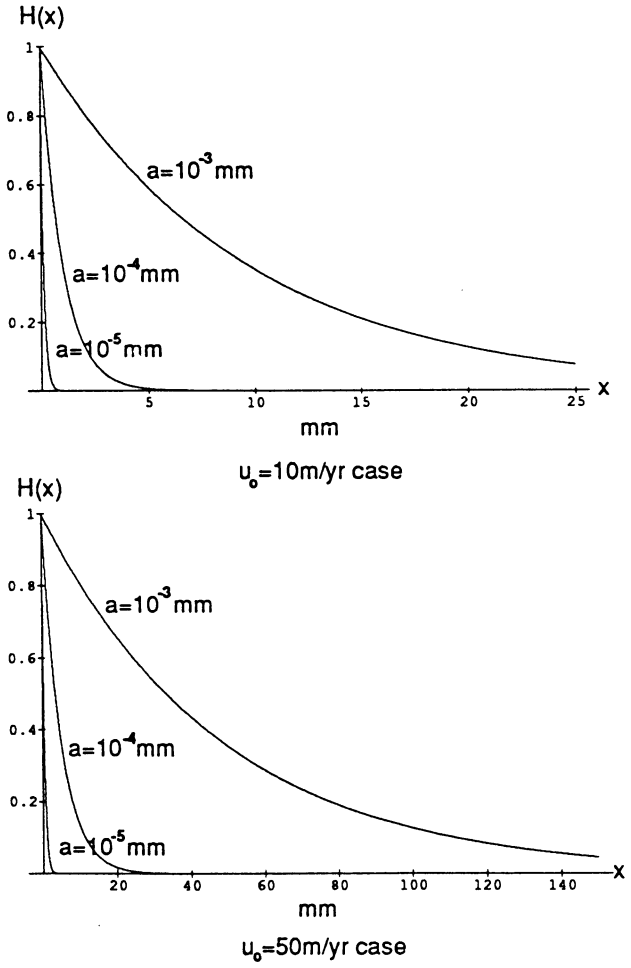

Figure 4: $H(X)$; the fraction of colloids sorbed at a distance greater than X along the fracture.

Consider an alternative scenario with a semi-infinite fracture ($x > 0$) and colloids continuously supplied at a known concentration at the inlet ($x = 0$). The corresponding solution of (7) is given by [6], viz.

$$c = \frac{c_0}{2}\left\{\exp\left(\frac{x(u^* + \sqrt{u^{*2} + 4D^*s^*})}{2D^*}\right)\operatorname{erfc}\left(\frac{x}{\sqrt{4D^*t}} + \frac{\sqrt{tu^{*2}D^* + 4s^*D^{*2}t}}{2D^*}\right)\right.$$
$$\left. + \exp\left(\frac{x(u^* - \sqrt{u^{*2} + 4D^*s^*})}{2D^*}\right)\operatorname{erfc}\left(\frac{x}{\sqrt{4D^*t}} - \frac{\sqrt{tu^{*2}D^* + 4s^*D^{*2}t}}{2D^*}\right)\right\}.$$

As $t \to 0$, this approaches the steady state

$$c = c_0 \exp\left(\frac{x(u^* - \sqrt{u^{*2} + 4D^*s^*})}{2D^*}\right).$$

Now consider the fraction $G(X)$ of colloids which penetrate to a distance greater than X. We have

$$G(X) = \exp\left(\frac{X(u^* - \sqrt{u^{*2} + 4D^*s^*})}{2D^*}\right).$$

In figure 5, we depict the behaviour of G for the parameters used previously in figure 4. Clearly there is a close agreement between figures 4 and 5. In fact

$$H(X) = \frac{1}{2 + 2\nu(1 - \sqrt{(1 + 1/\nu)})}G(X)$$

where $\nu = u^{*2}/4Ds^*$. Hence future calculations should utilize the more simple form $G(X)$. The difference between the two lies in the source. In the calculation of H, some colloids may diffuse back along the fracture, from $x = 0$, against the fluid flow, whereas such behaviour is not considered in the calculation of G.

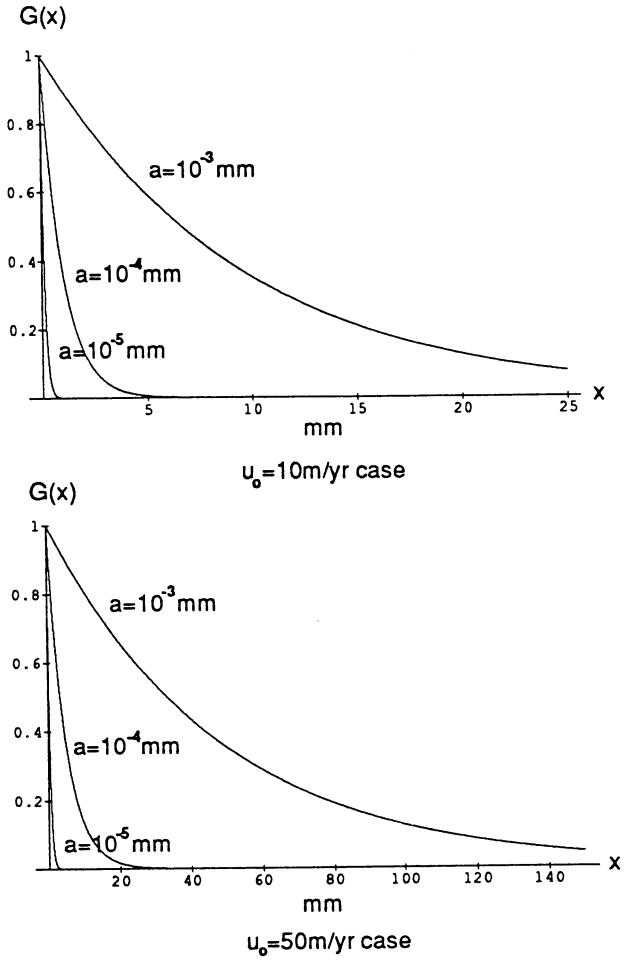

Figure 5: $G(X)$; the fraction of colloids which penetrate to a distance greater than X along the fracture.

Individual colloids do not migrate over large distances (> a few centimetres) given the parameter values used here. When $v \not\equiv 0$ and a repulsive force (due to surface charges) exists, colloids will migrate further.

Figures 4 and 5 should not be interpreted as an indication that colloids are not an effective medium in the dispersal of radionuclides. Rather it represents the penetration of individual colloids.

Natural colloids may migrate, become sorbed to the rock face, get released by hydrodynamic scouring, migrate, and so on. The effect would be a constant supply of colloids along the fracture with each colloid migrating according to processes reflected in figure 5. The effect is to provide an alternative means of transport for sorbing/desorbing nuclides, shifting from colloid to solute to colloid. Whilst colloid bound, their macroscopic transport (dispersion, advection) is altered to that of colloids (for example,

an average flow rate 30% above that of the fluid).

Let $q(x,t)$ denote the supply rate of colloids per unit fracture length per year, then (7) becomes

$$c_t = D^* c_{xx} - u^* c_x - s^* c + q. \tag{8}$$

Our aim is to include the colloid behaviour, illustrated above, in a nuclide-colloid fracture migration model in section 3.

Such problems have recently been considered in [11] and it is constructive to discuss the treatment of colloid dispersion, migration and sorption in the light of that approach and its data requirements. We shall consider the associated nuclide-colloid interactions elsewhere.

In [11], the macroscopic colloid transportation model is a one-dimensional fracture (cf. (7) above) and must assume values for colloid dispersion coefficients (D^* here), and the colloid flow rates (u^*).

It is possible to avoid an explicit consideration of colloid sorption rates by introducing an empirical partition coefficient representing the constant fraction of sorbed colloids.

Clearly our derived values for D^* and u^* could be utilized in the subsequent analysis employing these models. In [11], no attempt is made to suggest the dependencies of the parameters upon colloid size, composition or fracture transmissivity. In our present model, by taking g constant and allowing (8) to equilibrate, we obtain a colloid migration situation analogous to that of [11]. We obtain

$$c \equiv c_0, \text{ say,}$$

$$\text{where } q_0 = c_0 s^*.$$

Thus radionuclide migration may be considered against the background of a constant ambient colloid population of individuals dispersing according to the processes derived above.

The important fact is that rather than assume values for dispersivity, flow rates, sorption rates and equilibrium constants on the basis of experience, experiment and expectation, we have been able to derive estimates depending upon the quantitative microscopic physical and chemical processes at work.

2.4 Experimental data

Although we have considered a planar fracture, similar calculations can be made for a fracture having a uniform circular cross-section. Clearly there would be much utility in performing laboratory experiments employing capillary tubes; well documented, uniform (perhaps synthetic) colloids; slow pump rates. The colloid radii should be varied over a number of experiments, as could the surface charges, the water chemistry, the flow rates, and fracture apertures. Some such data may already be available in the form of hydrodynamic chromatography employing porous capillary membranes.

Such experiments and data could be used to validate the theoretical model presented here, and refine the predictions made on both the laboratory and field scales of space and time.

The method deployed in [10] and this report could be used to analyse experimental data from hydrodynamic chromatography [5]. In such experiments (and generalisations [7]), colloids and larger particles are dispersed in fluid pumping through a capillary tube. There is no adsorption at the capillary faces, though repulsive surface charges may be present. Hence the particles flow through at a rate close to that of the fluid. Typical experiments measure a retention factor R_f defined by

$$R_f = \frac{\text{mean flow rate of particles}}{\text{mean flow rate of fluid}} = \frac{\text{transit time for fluid}}{\text{transit time for particles}}.$$

Using the asymptotic spectral comparison method [10], we may calculate R_f values, given that particles at a distance r from the centre of the capillary are advected at a rate $v(r)$ towards the capillary surface, at $r = r_0$.

We obtain

$$R_f = \frac{2\int_0^{r_0-a}(1-\frac{r^2}{r_0^2})r\tilde{f}(r)\,dr}{\int_0^{r_0-a} r\tilde{f}(r)\,dr}$$

where

$$\tilde{f}(r) = e^{\int_0^r v(\tilde{r})/D\,d\tilde{r}}.$$

Here a is the particle radius; D is the diffusivity, given by (2); and the fluid flow rate is proportional to $(1 - r^2/r_0^2)$.

An experimental calibration curve is given in [5]. If $v \equiv 0$

$$R_f = \left(2 - \left(\frac{r_0 - a}{r_0}\right)^2\right)$$

which is well below the observed curve.

In order to illustrate the effect of surface forces we set

$$v = -v_0 r,$$

where $v_0 > 0$ represents advection due to a repulsive force falling off linearly to zero as the particle approaches $r = 0$.

We obtain

$$R_f = 2 - \frac{4D}{v_0 r_0^2} + \frac{(r_0 - a)^2}{r_0^2} \frac{2}{\exp(\frac{v_0}{2D}(r_0 - a)^2) - 1)}.$$

For values of v_0 between 2 and 20 mm/yr the corresponding behaviour of R_f, as a function of colloid radius, is depicted in figure 6.

More analysis along these lines, with realistic functions $v(r)$, could be undertaken, possibly in collaboration with hydrodynamic chromatography expertise.

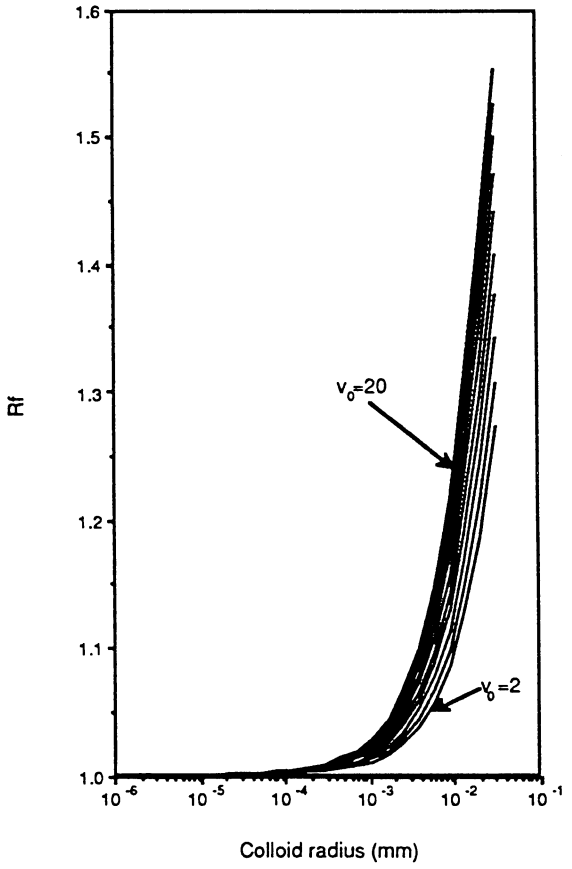

Figure 6: R_f as v_0 varies.

Almost all previous colloid migration experimental programmes have concentrated on the advection, dispersal and sorption of colloids in packed columns, an early example being [1]. Indeed it is likely that the major experimental work carried out in the next phase of the CEC MIRAGE programme will again be dominated by column experiments.

However, available results and the application of filtration-type theories suggest that such porous media provide an effective barrier to colloid transport. Hence our present emphasis on fracture flow. For more convoluted or tortuous fractures, capillaries, or pores, the microscopic model remains unchanged: we should merely specify a more complex geometry. Of course some effort would be required to obtain the dynamic parameters valid on the larger scale in an analogous manner to the theory developed here.

A further experimental issue is the identification of the relevant surface forces. Recent results [8] have suggested the inadequacy of DLVO-type theories when applied on the scale of nanometres. As this debate continues we are free to recalculate the parameters of this section, substituting in any preferred functional form for the advection due to surface forces ($v(z)$ in (1)). Colloid and surface science is an active and developing field, and our modelling approach has allowed for such fundamental considerations to be included at the first stage.

Overall the results of this section are in harmony with the conceptual and experimental view of colloid migration. Surface forces, and size keep colloids more centre-stream than solutes. The consequence is an increase in their average advection and a decrease in their hydrodynamic dispersion. We have also made predictions for sorption rates and individual migration.

3 Radionuclide-Colloid migration modelling

3.1 A radionuclide transport model

Here we shall define a nuclide migration model, taking account of the effect of a background population of colloids within a planar fracture.

We shall assume that colloids are either free, being advected downstream within the fracture, or stationary, sorbed to the rock faces. Such colloids will be assumed to have equilibrated, so that the rate at which free colloids become sorbed is balanced by the source term, q (see below), representing the release of stationary colloidal material into the fracture.

The geometrical set-up is shown in figure 7. Radionuclides are present in one of the following ways:

- free, in solute form within the fracture;
- sorbed to free colloids;
- sorbed to stationary colloids;
- in solute within the water-filled pore space;
- sorbed to the rock mass, in equilibrium with the concentration within the pore space.

As in other standard radionuclide transport models, we shall allow the solute present within the porous rock to diffuse only in the z direction, perpendicular to the fracture plane, see figure 7. We begin by assuming that the colloids are of uniform size, with radius a, say.

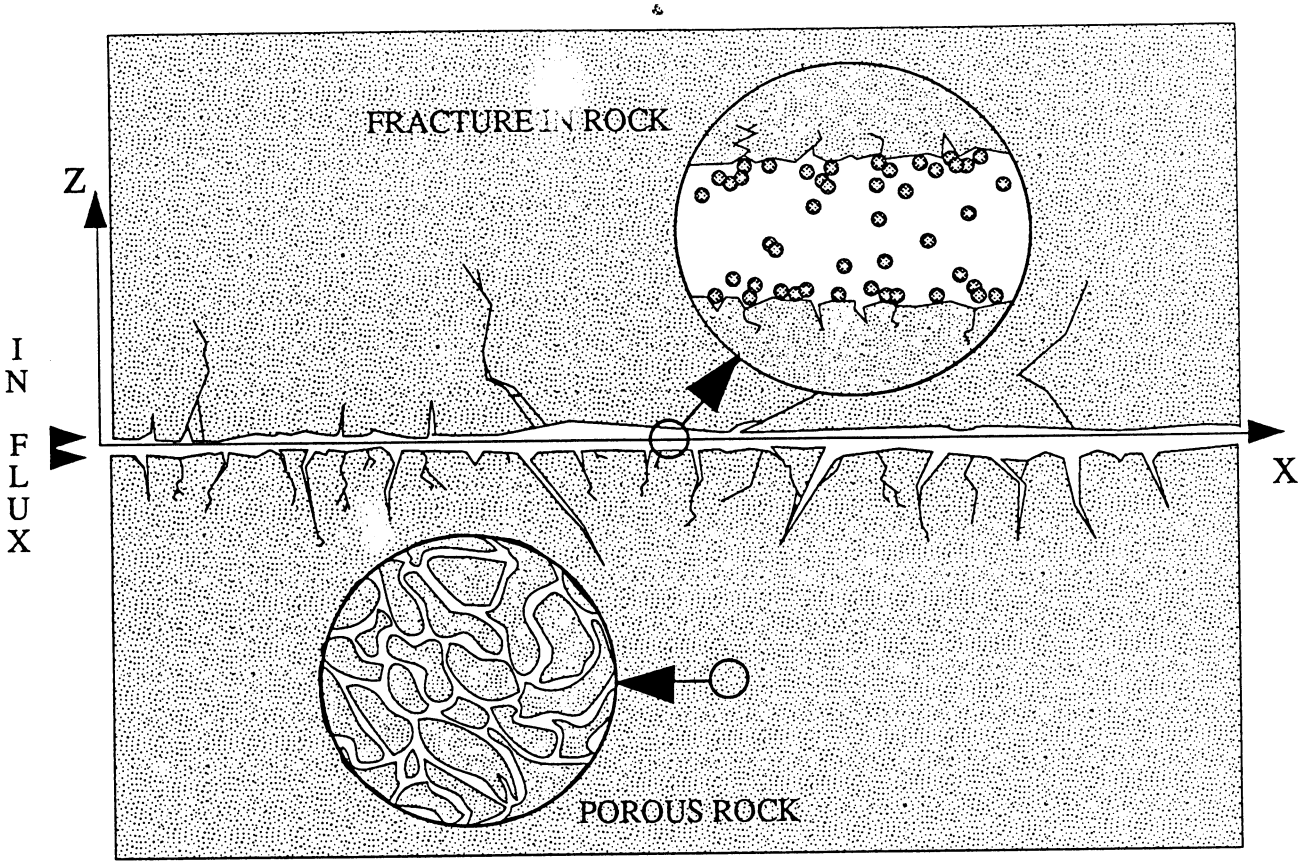

Figure 7: The fracture zone

Let us define

$c(x,t)$ density of free colloids present within the fracture (colloids per unit volume);

$d(x,t)$ density of immobile colloids present within the fracture (colloids per unit fracture volume);

$w(x,z,t)$ concentration of radionuclides in solution within the fracture (mols per unit fracture volume);

$W(x,z,t)$ concentration of radionuclides in solution within the pore space (mols per unit rock mass volume);

$v(x,t)$ concentration of radionuclides bound to free colloids within the fracture (mols per unit fracture volume);

$p(x,t)$ concentration of radionuclides bound to immobile colloids within the fracture (mols per unit fracture volume).

Let $q(d)$ denote the rate at which colloids are released from the immobile colloidal mass into the fracture. Conservation of mass, along with the one-dimensional colloid migration model developed in section 2, imply

$$
\begin{aligned}
c_t &= D^* c_{xx} - u^* c_x - s^* c + q(d) \\
d_t &= s^* c - q(d) \qquad\qquad (9) \\
&\qquad\qquad x \geq 0, \quad t > 0
\end{aligned}
$$

Here D^*, u^* and s^* are as defined in section 2. In addition, we now include the source term $q(d)$. The system (9) is assumed to be in equilibrium on the timescale associated with radionuclide release, transport and dispersal. Hence we have

$$c \equiv c_0 \qquad \text{and} \qquad d \equiv d_0$$

where $s^* c_0 = q(d_0)$. Note that $\frac{4}{3}\pi \rho_{\text{mat}} a^3 c_0$ is the total mass per unit volume of free colloids within the fracture (of radius a and material density ρ_{mat}). So far, we have not discussed $q(d)$ explicitly, but we shall return to its effect later.

Let $g_1(v)$ denote the rate per unit volume at which nuclides become unsorbed from free colloids and released into solution (mols per unit fracture volume per unit time). Let $g_2(p)$ denote the rate per unit volume at which nuclides become unsorbed from immobile colloids and released into solution, (mols per unit fracture volume per unit time).

Let $s_1(c_0, w)$ and $s_2(d_0, w)$ denote the rates per unit volume at which nuclides in solution become sorbed to free and immobile colloidal surfaces respectively (mols per unit fracture volume per unit time).

Let $\tilde{q}(p, v, d_0)$ denote the rate at which nuclides are exchanged between immobile and free colloids as a consequence of instantaneous colloidal rock sorption or release. From our earlier constructions, it is clear that

$$\tilde{q}(p, v, d_0) = s^* v - q(d_0)\frac{p}{d_0}, \qquad (10)$$

since $\frac{p}{d_0}$ denotes the average mass of nuclides sorbed to each colloid and s^* and $q(d_0)$ are defined in (9).

Using the above terms, together with (9), and employing a standard dispersion theory argument for the solute within the fracture, we obtain

$$
\begin{aligned}
w_t &= \tilde{D} w_{xx} - \tilde{u} w_x + \frac{\phi D}{L} W_z - \lambda w \\
&\qquad -s_1(c_0, w) - s_2(d_0, w) + g_1(v) + g_2(p), \qquad (11) \\
v_t &= D^* v_{xx} - u^* v_x - \lambda v - \tilde{q}(p, v, d_0) + s_1(c, w) - g_1(v), \qquad (12) \\
p_t &= -\lambda p + \tilde{q}(p, v, d_0) - g_2(p) + s_2(d_0, w), \qquad (13) \\
&\qquad\qquad x > 0, \quad t > 0.
\end{aligned}
$$

Here ϕ denotes the porosity of the rock; D denotes the molecular diffusivity of the solute with the pore water; L is the half fracture width, as before; $\tilde{D}$ denotes the effective diffusivity of the solute, including standard Taylor dispersion within the fracture (see the Appendix); $\tilde{u}$ is the cross-fracture average fluid velocity; and λ is the decay rate of the nuclide. For simplicity, we have considered a single nuclide decay chain: the generalization being obvious. D^*, u^* and s^* are as defined in section 2 and (9).

Now (9) must be solved in conjunction with

$$RW_t = DW_{zz} - R\lambda W, \qquad z > 0, \quad x > 0, \quad t > 0. \tag{14}$$

Here R is the retardation of the nuclide in the porous rock. At $z = 0$, we have continuity of concentration:

$$W(0, x, t) = w(x, t), \qquad t \geq 0.$$

Adding (11), (12) and (13), we obtain

$$w_t + p_t + v_t = \tilde{D}w_{xx} + D^*v_{xx} - \tilde{u}w_x - u^*v_x - \lambda(w + p + v) + \frac{\phi D}{L}W_z, \tag{15}$$

Now assuming that the equilibrium of nuclides within the fracture between solute and colloid-bound states occurs on a scale fast compared to that associated with their transport and dispersal, we shall employ (15) instead of (11)-(13), along with the linear partitions

$$\begin{aligned} v &= k_1 w, \\ p &= k_2 w, \end{aligned} \tag{16}$$

describing this pseudo equilibrium, valid at low concentrations of colloids (free and sorbed). The relationship between k_1, k_2 and the terms s_1, s_2, g_1, g_2 and $\tilde{q}$ is discussed below in subsection 3.2.

Using this simplification, (15) becomes

$$\begin{aligned} (1 + k_1 + k_2)w_t &= (\tilde{D} + k_1 D^*)w_{xx} - (\tilde{u} + k_1 u^*)w_x \\ &\quad -\lambda(1 + k_1 + k_2)w + \frac{\phi D}{L}W_z, \\ &\quad x > 0, \quad t > 0. \end{aligned} \tag{17}$$

We shall solve (17) together with (14), imposing suitable initial and boundary conditions at $x = 0$, $x \to \infty$, $z \to \infty$, and $t = 0$.

3.2 Partition Coefficients

In order to motivate the definition of the linear partition coefficients k_1 and k_2 in (16), we proceed as follows.

We assume that the nuclides reach a local equilibrium distribution between solute and free and immobile colloid-bound species on a fast timescale relative to that of the transport and dispersal processes. Thus in (11), (12) and (13), we have

$$\begin{aligned} s_1(c_0, w) &= g_1(v) + \tilde{q}(p, v, d_0) \\ s_2(d_0, w) &= g_2(p) - \tilde{q}(p, v, d_0) \end{aligned} \tag{18}$$

Without this assumption, (15) is still valid but cannot be reduced to a single equation in one unknown (c.f. (17)).

The terms s_1 and s_2 depend upon the local concentration of nuclides, w, and the available sorption sites on the colloidal surfaces, for populations c_0 and d_0 respectively.

In [10], it is suggested that such interactions have the form

$$\begin{aligned} s_1(c_0, w) &\approx \eta_1 4\pi a^2 c_0 w, \\ s_2(d_0, w) &\approx \eta_2 4\pi a^2 d_0 w. \end{aligned} \tag{19}$$

Here $4\pi a^2 c_0$ denotes the free colloid surface area per unit fracture volume, and η_1 denotes the sorption rate of nuclides per unit area of free colloidal surface. Similarly, $4\pi a^2 d_0$ and η_2 for immobile colloid-nuclide sorption.

Note that if s_1 is written in terms of free colloid mass density (colloidal mass per unit fracture volume), $\rho_{\text{col}} = \frac{4}{3}\pi\rho_{\text{mat}} a^3 c_0$, then we obtain

$$s_1 \approx \eta_1 \frac{3\rho_{\text{col}}}{a\rho_{\text{mat}}} w$$

so that the analogue of the usual K_d is inversely proportional to the colloid radius.

Using (10), (19) and (20) in (18) and (19), we obtain

$$\begin{aligned} \eta_1 4\pi a^2 c_0 w &= g_1(v) + s^* v - \frac{q(d_0)}{d_0} p \\ \eta_2 4\pi a^2 d_0 w &= g_2(p) - s^* v + \frac{q(d_0)}{d_0} p. \end{aligned}$$

Next expand $g_1 = g_1^* v + O(v^2)$ and $g_2 = g_2^* + O(v^2)$ and we obtain to first order a linear system for v and p valid at low colloid concentrations. This last yields

$$\begin{aligned} v &= \frac{4\pi a^2 w}{(g_1^* g_2^* + s^* g_2^* + \frac{q(d_0)}{d_0} g_1^*)} \Big[c_0 \eta_1 [\frac{q(d_0)}{d_0} + g_2^*] + d_0 \eta_2 \frac{q(d_0)}{d_0} \Big], \\ p &= \frac{4\pi a^2 w}{(g_1^* g_2^* + s^* g_2^* + \frac{q(d_0)}{d_0} g_1^*)} \Big[c_0 \eta_1 s^* + d_0 \eta_2 (s^* + g_1^*) \Big]. \end{aligned}$$

Thus comparing with (16), we have

$$k_1 = \frac{4\pi a^2 \Big(c_0 \eta_1 (\frac{q(d_0)}{d_0} + g^*) + \eta_2 q(d_0) \Big)}{\Big(g_1^* g_2^* + s^* g_2^* + \frac{q(d_0)}{d_0} g_1^* \Big)}, \tag{20}$$

$$k_2 = \frac{4\pi a^2 \Big(c_0 \eta_1 s^* + d_0 \eta_2 (s^* + g_1^*) \Big)}{\Big(g_1^* g_2^* + s^* g_2^* + \frac{q(d_0)}{d_0} g_1^* \Big)}. \tag{21}$$

Note, by hypothesis, $s^* c_0 = q(d_0)$.

If $q(d_0) \equiv q_0 d_0$ is linear, then these simplify to become

$$k_1 = \frac{4\pi a^2 c_0 \Big(\eta_1 (q_0 + g_2^*) + \eta_2 s^* \Big)}{\Big(g_1^* g_2^* + s^* g_2^* + q_0 g_1^* \Big)}, \tag{22}$$

$$k_2 = \frac{4\pi a^2 c_0 \Big(\eta_1 s^* + \frac{s^*}{q_0} \eta_2 (s^* + g_1^*) \Big)}{\Big(g_1^* g_2^* + s^* g_2^* + q_0 g_1^* \Big)}. \tag{23}$$

4 Model Calculations

In order to assess the effect of colloids upon the migration and dispersal, we consider the following system (14), (17) which was derived in the last section:

$$\begin{aligned}
(1+k_1+k_2)w_t &= (\tilde{D}+k_1D^*)w_{xx} - (\tilde{u}+k_1u^*)w_x \\
&\qquad -\lambda(1+k_1+k_2)w + \frac{\phi D}{L}W_z \\
&\qquad x>0, \quad t>0, \\
RW_t &= DW_{zz} - R\lambda W \\
&\qquad z>0, \quad t>0.
\end{aligned} \tag{24}$$

$$\begin{aligned}
W \to 0 \quad &\text{as} \quad z \to \infty \quad x>0 \quad t>0, \\
W,\ w \to 0 \quad &\text{as} \quad x \to \infty \quad t>0, \\
W(x,0,t) &= w(x,t) \quad x>0 \quad t>0, \\
w(x,0) &\equiv 0 \quad x>0, \\
W(x,z,0) &\equiv 0 \quad x>0 \quad z>0.
\end{aligned}$$

At $x=0$, we impose the boundary condition

$$h(t) = \left[\begin{array}{c}\text{flux of radionuclides} \\ \text{into the fracture}\end{array}\right] = (\tilde{u}+k_1u^*)w - (\tilde{D}+k_1D^*)w_x$$

where h is given. For simplicity, we begin by taking

$$h(t) = h_0e^{-\lambda t}.$$

A measure of the natural barrier afforded by the fracture, the colloids, and the porous rock is given by the breakthrough flux of nuclides through the fracture at a distance x_0 along the fracture. Thus we shall observe the time dependent behaviour of the normalized flux down the fracture at $x=x_0$, given by

$$f(t) = \frac{1}{h_0}\Big\{(\tilde{u}+k_1u^*)w(x_0,t) - (\tilde{D}+k_1D^*)w_x(x_0,t)\Big\}.$$

Note that the constant h_0 scales $h(t)$ so that $f(t)$ represents the flux through the fracture, at $x=x_0$, given the corresponding normalized influx

$h(t)/h_0$. Of the parameters employed in (24), k_1 and k_2 are the least certain. They can be defined by

$$\frac{k_1}{1+k_1+k_2} = \text{fraction of nuclides within the fracture sorbed to free colloids}$$

$$\frac{k_2}{1+k_1+k_2} = \text{fraction of nuclides within the fracture sorbed to immobile colloids.}$$

Alternatively, they are given in the previous subsection as functions of known microscopic parameters and (currently uncertain) sorption rates. Given this uncertainty, we shall allow k_1 and k_2 to vary over four orders of magnitude each. For each pair of values, we obtain a breakthrough curve. Note that $k_1 = k_2 = 0$ represents the no colloids case.

Employing the Laplace transform, we solved this problem in the Laplace domain to yield the transform, $\hat{f}$, of f. Next we inverted by using a numerical algorithm due to Talbot [15]. This has been extensively used and verified for similar calculations over a number of years [19] . We made all our numerical calculations employing a symbolic mathematics package able to work to any specified precision. This also provided the graphical output. Calculations were verified against existing Fortran codes for Talbot's method.

The remaining parameter values employed are given in table 4. Before examining the results, we briefly discuss their selection.

L	10^{-4}m
D	10^{-3}m^2/yr
$\tilde{D}$	10^{-3}m^2/yr
D^*	10^{-4}m^2/yr
$\tilde{u}$	10m/yr
u^*	13.5m/yr
ϕ	10^{-4}
R	10
λ	10^{-4}yr^{-1}
x_0	1000m

Table 4: Parameter Values

We choose L and $\tilde{u}$ so as to be commensurate with the earlier calculations in section 2. The values for D^* and u^* follow assuming that the

colloids have radii $\approx$ 100nm, and that there are relatively large surface forces keeping free colloids centre stream (v_0 large in figure 3). This is the conservative assumption maximising the effect of the free colloids upon nuclide migration along the fracture.

For particles in solute, a molecular diffusivity of $10^{-3}\mathrm{m}^2/\mathrm{yr}$ is of the correct order. Following the Appendix, the corresponding Taylor dispersivity is of order $10^{-5}\mathrm{m}^2/\mathrm{yr}$. Thus we take $\tilde{D} = D$ in these calculations. A decay rate of $10^{-4}\mathrm{yr}^{-1}$ is long enough so as not to have any large effect upon the breakthrough behaviour, which occurs around 100 years, for x_0 given by 1000m.

The retardation, R, is given by

$$1 + \frac{\rho_{\mathrm{rock}} K_d (1-\phi)}{\phi}$$

where ρ_{rock} is the density of rock material, ϕ is the porosity and K_d is the usual sorption partition coefficient.

The breakthrough behaviour is highly sensitive to ϕ.

For the values given in table 4, our results are shown in figures 8 (a)-(e). In figures 8 (b)-(e), we fixed $k_2 = 0.001, 0.01, 0.10, 1.00$ respectively, whilst k_1 was varied. Figure 8(a) depicts 14 out of the total of 16 breakthrough curves. We also show the *no colloid*, $k_1 = k_2 = 0$, base case.

In figure 9 (a)-(e) we depict the total concentration of nuclides per unit fracture volume as functions of time at $x = x_0$. This includes nuclides present in solution and bound to free and immobile colloids. Again the breakthrough curves are plotted as k_1 and k_2 vary over four orders of magnitude independently.

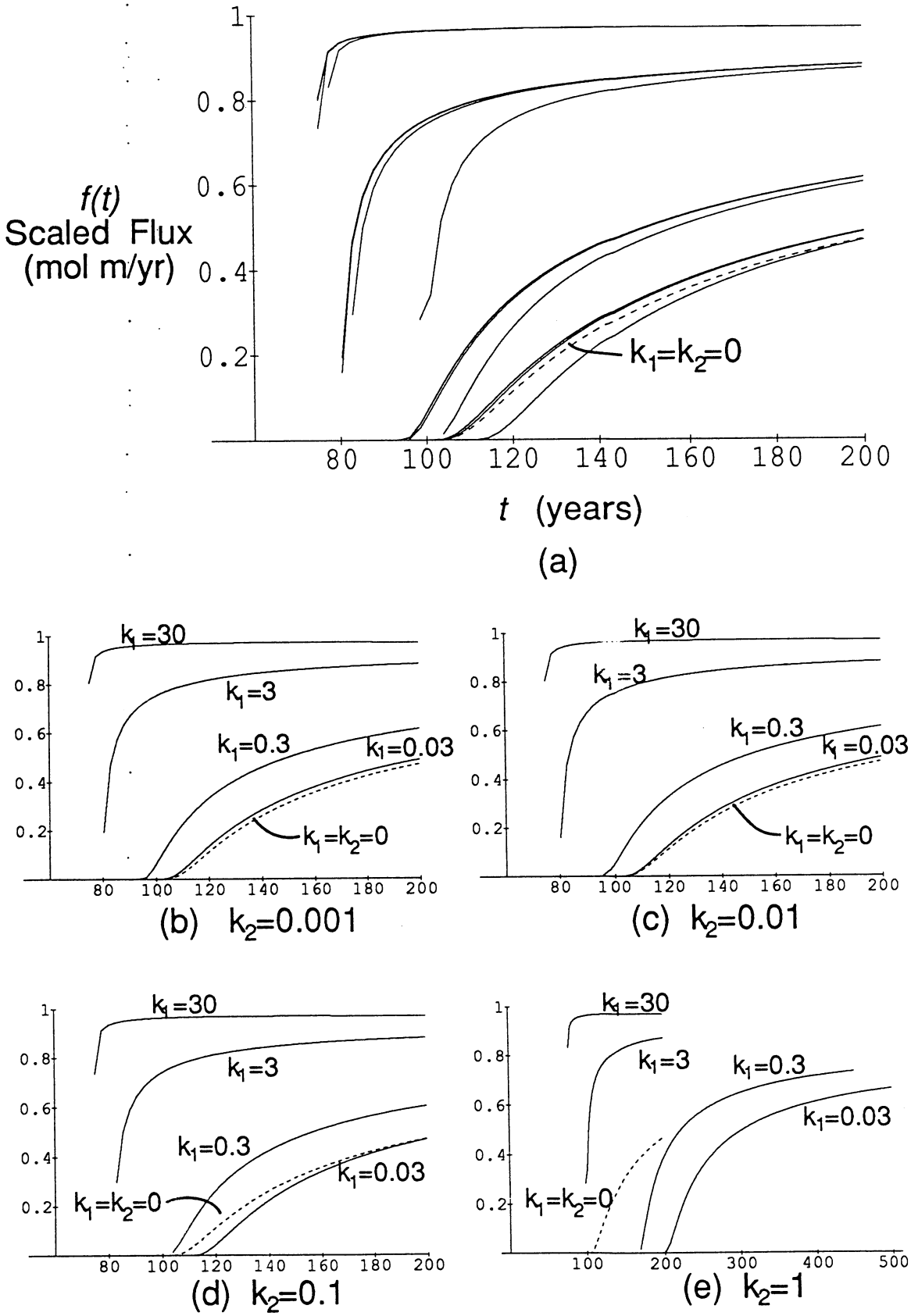

Figure 8: Breakthrough curves for k_1 and k_2 varying

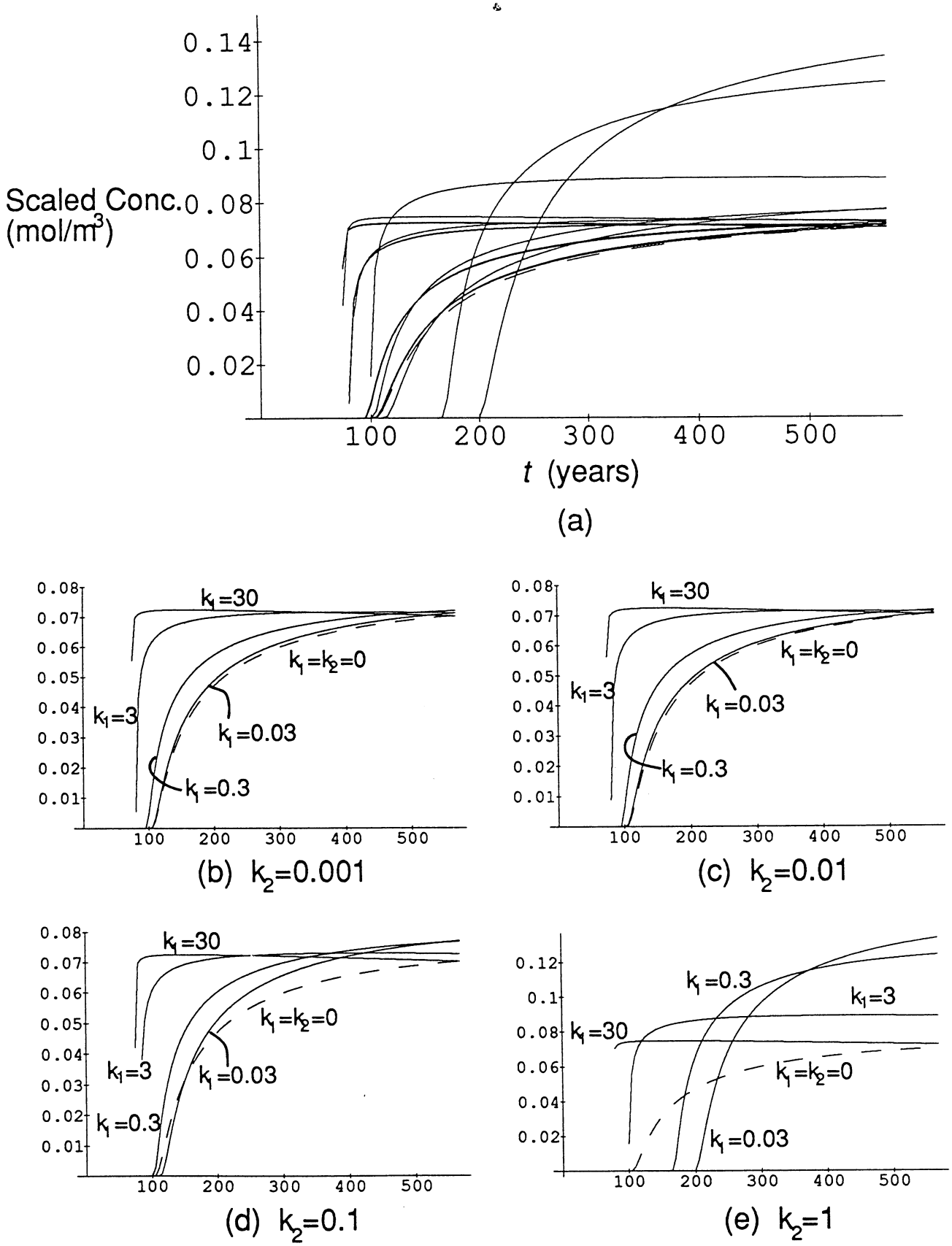

Figure 9: Concentration breakthrough curves for k_1 and k_2 varying

5 Further Applications

Calculations of breakthrough curves, such as those in the previous section, could be made for a range of scenarios. In particular, here we shall discuss the effect of

- an inhomogeneous background population of colloids
- dissolution of true colloids supplied, together with the solute at the fracture inlet.

The breakthrough curve for radionuclides in the absence of colloids has been observed to lie between the extreme cases postulated for radionuclide-colloid sorption equilibria. These are given by large k_1 and small k_2, and large k_2 and small k_1, respectively. By allowing the partition coefficients to vary independently over four orders of magnitude we have illustrated the sensitivity of the results to their possible chosen values.

Clearly it would be desirable to integrate such calculations within the Geosphere cases to be produced for Project 90. By choosing commensurate physical and geochemical parameters the variability of breakthroughs with respect to background levels of colloids could be assessed.

Having made test calculations based upon uniform, steady-state, populations of free and immobile colloid material, we examine two alternative model scenarios.

5.1 Inhomogeneous colloid distributions

Here, as before, we assume that colloids are supplied to, and captured from, the fracture reaching equilibrium in (9) (section 3.1) between the free and immobile states. That is

$$s^* c \equiv q(d). \tag{25}$$

We also assume that there is an increased influx of colloidal material at the fracture inlet due to the presence of the repository. The resulting distributions for c and d are no longer independent of space and time. We solve

$$\begin{aligned} c_t &= D^* c_{xx} - u^* c \quad x > 0,\ t > 0, \\ c(x,0) &= c_\infty \qquad\qquad x > 0, \\ c(0,t) &= c_1 \qquad\qquad t > 0, \end{aligned}$$

where c_∞ and c_1 are constants representing the background constant level of free colloids (prior to the commencement of the repository source term at $t = 0$), and the increased in flow concentration of colloids supplied at the inlet (for $t > 0$).

We have

$$c(x,t) = c_\infty + \frac{(c_1 - c_\infty)}{2}\left\{\exp\left(\frac{xu^*}{D^*}\right)\mathrm{erfc}\left(\frac{x}{\sqrt{4D^*t}} + \sqrt{\frac{tu^*}{4D^*}}\right) + \mathrm{erfc}\left(\frac{x}{\sqrt{4D^*t}} - \sqrt{\frac{tu^*}{4D^*}}\right)\right\}. \quad (26)$$

This in turn defines $d(x,t)$, via (25).

The inhomogeneity in colloid distribution within the fracture directly affects the radionuclide migration model (24) through the definition of the partition coefficients, k_1 and k_2. For simplicity we assume $q(d)$ is linear so that k_1 and k_2 are given by (22) and (23) respectively, with c_0 replaced by $c(x,t)$ from (26), (if $q(d)$ were nonlinear k_1 and k_2 would be given by (20) and (21) with c_0 replaced by $c(x,t)$).

Then it is clear that k_1 and k_2 are both proportional to $c(x,t)$, say

$$k_1 = \tilde{k}_1 c(x,t), \quad (27)$$

$$k_2 = \tilde{k}_2 c(x,t), \quad (28)$$

where $\tilde{k}_1$ and $\tilde{k}_2$ are constants. We may seek to solve (24) with spatially and temporarily inhomogeneous coefficients k_1 and k_2. Without loss of generality we may absorb c_1 into $\tilde{k}_1$ and $\tilde{k}_2$ and use (27) and (28) together with

$$c(x,t) = \frac{c_\infty}{c_1} + \left(1 - \frac{c_\infty}{c_1}\right)\left\{\exp\left(\frac{xu^*}{D^*}\right)\mathrm{erfc}\left(\frac{x}{\sqrt{4D^*t}} + \sqrt{\frac{tu^*}{4D^*}}\right) + \mathrm{erfc}\left(\frac{x}{\sqrt{4D^*t}} - \sqrt{\frac{tu^*}{4D^*}}\right)\right\}.$$

This indicates that we now have three degrees of freedom: $\tilde{k}_1$, $\tilde{k}_2$, and the ratio c_∞/c_1, which must be specified in any approach to the radionuclide migration problem.

The resulting equations are no longer amenable to solution via Laplace transform methods owing to the non-constancy of the coefficients in (24). Nevertheless it remains linear and we shall solve it using appropriate techniques in the next phase of the SKI Radionuclide-Colloid Migration Initiative if appropriate.

5.2 The migration of true colloids

Thus far we have sought to model systems where the colloid material, whatever its source, was conserved, with radionuclides coming from solution to sorb to colloid surface sites. This implicitly includes all pseudo-colloid migration scenarios.

An area where this assumption is less valid is the dispersal of true colloids: aqueous colloids formed from the nucleation of radionuclides.

The formation of such colloids would require supersaturation of the dissolved species in a neighbourhood of the source term. In field studies anomalous rapid transport of radionuclides has occasionally been observed. In [18] instances are cited where Pu and Am migrated over a distance of 30m through unsaturated tuff in 30 years.

In order to utilize the results of section 2 to model the dispersal of true colloids, we suppose that true colloids are supplied at the fracture inlet, along with an unsaturated level of the dissolved species. The true colloids are dispersed within the fracture according to (9), with the additional caveat that the colloids dissolve, becoming smaller and smaller. Strictly the rate of dissolution depends upon the local level dissolved concentration, and we envisage including such effects in future modelling and calculations.

Here we shall simplify matters by assuming that the rate of dissolution is effectively constant, so that an individual colloid is decreased in volume at a rate proportional to its surface area. Consider a spherical colloid, of radius $a(t)$ then

$$\frac{d(4/3\pi a^3)}{dt} \propto 4\pi a^2 L$$

Thus $\frac{da}{dt}$ is constant.

Consider a population of such colloids, with initial radius $a = a_0$, supplied within an infinite fracture at $x = 0$, at time t.

We consider

$$\begin{aligned} c_t &= D^*(a)c_{xx} - u^*(a)c_x - s^*(a)c + q(d), \\ d_t &= s^*c - q_0(d) \quad -\infty < x < \infty,\ 0 < t < \frac{a_0 - a_s}{\mu}, \\ \text{where } a &= a_0 - \mu t. \end{aligned}$$

Here we assume that the decay rate of the actinide is small so as to concentrate on the colloid dispersal mechanism; μ is a constant determining the rate of dissolution of the colloids, and $t = (a_0 - a_s)/\mu$ represents the

time at which the colloids become completely dissolved, when $a = a_s$ the radius of a single radionuclide. Let us assume local equilibrium between the free and immobile colloids within the fracture so that we have

$$d \equiv kc.$$

Then we may solve

$$(1+k)c_t = D^*(a)c_{xx} - u^*(a)c_x, \tag{29}$$

$$a = a_0 - \mu t, \quad -\infty < x < \infty, \; 0 < t < \frac{a_0 - a_s}{\mu}, \tag{30}$$

with $c(x,0) = \delta(x)$, the Dirac point mass centred at the origin.

We have a linear system with time dependant coefficients. This problem may be solved via the Fourier transform method once $D^*(a)$ and $u^*(a)$ are specified. We should choose appropriate forms which fit the curves derived in section 2, see figure 3.

Such calculations, and those for more sophisticated versions of the model could be made to estimate distances travelled by colloids prior to dissolution. Of course, the conservative case is given by $k = 0$ (no retardation due to fracture surface sorption), and $\mu = 0$ (no dissolution). We envisage completing such calculations in some detail in the future.

As an example, we solve (29) and (30) choosing $D^*(a) = 5.4 \times 10^{-12}/a$ (m/yr), $u^*(a) = 13 + (a - a_s)/(a_0 - a_s)$ (m/yr), $a_0 = 10^{-6}$ (m), $a_s = 5.4 \times 10^{-9}$ (m), $k = 0$, $\mu = (a_0 - a_s)/500$ (m/yr).

At $t = 500$ years, all of the colloids have radii $a = a_s$ (that of a single radionuclide). The distribution of such colloids represents the furthest penetration of true colloidal material within the fracture. Subsequent radionuclide migration will be in solute form, since all of the colloids have been dissolved away to individual radionuclides which henceforth disperse independently. We have

$$c(x,500) = \sqrt{\frac{\pi}{A}} e^{-(x+B)^2\pi^2/A},$$

where

$$A = \frac{4\pi^2 \tilde{D}}{\mu} \ln\left(\frac{a_0}{a_s}\right),$$

$$B = -6500 + \frac{500(a_0 - a_s + 25\mu)}{10^{-6} - a_s}.$$

This distribution may be compared directly with the corresponding distribution of radionuclides released at $x = 0$, and transported as true colloids

consisting of single nuclides (ie. effectively in solution), having $k = 0$, diffusivity $D^*(a_s)$ and advection $u^*(a_s)$. In figure 10 we depict both distributions. Since larger colloids are less hydrodynamically dispersed, and are advected further, the true colloids are seen to penetrate further through the fracture.

A fuller calculation is necessary to account for the subsequent soli transportation of the radionuclides dissolved from the true colloids. A ie colloids dissolve they provide a mobile source for the solute species. Hence we should complement the above calculation, which tracks a population of true colloids, with an equation for the simultaneous dispersion of the radionuclides in solution.

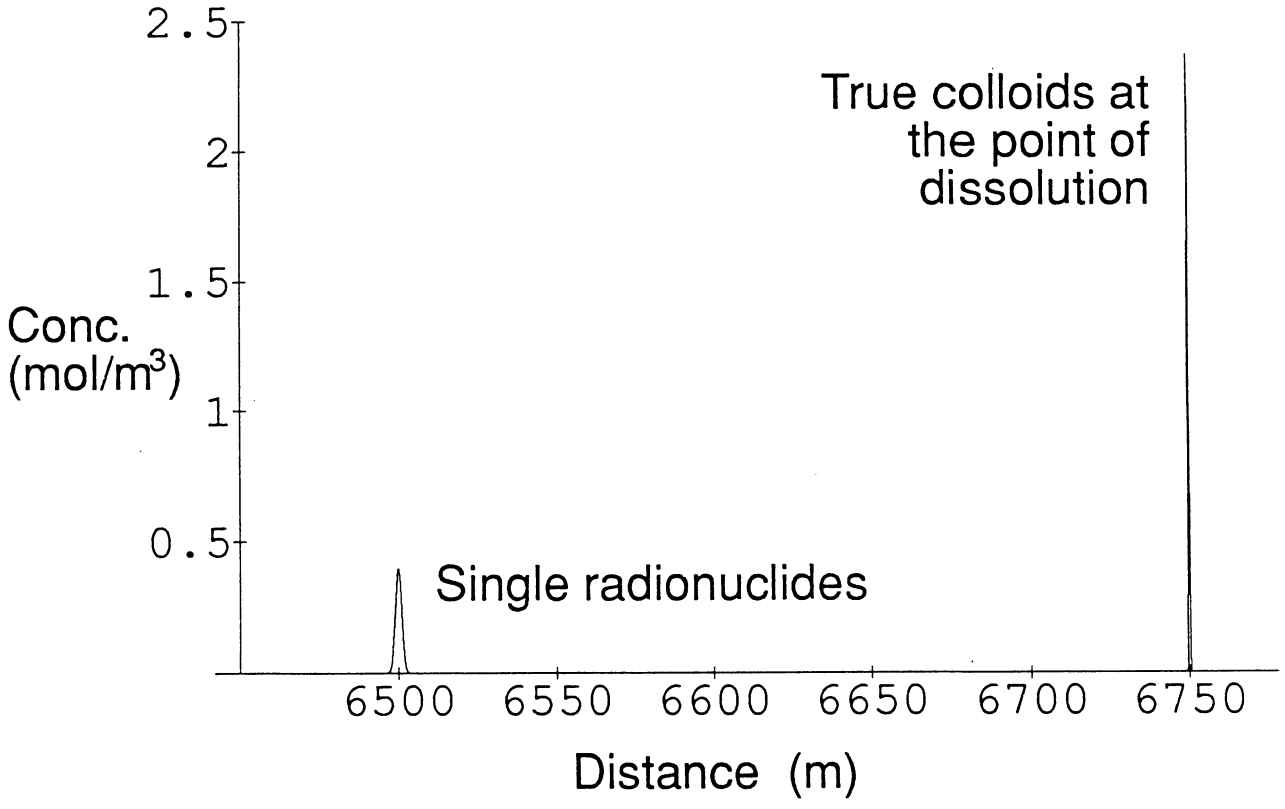

Figure 10: Distributions at $t = 500$

6 Summary

In this second phase of the SKI radionuclide-colloid migration project the model specified in Phase I has been further refined and calculations of radionuclide dispersal and transport were made assuming a background level of colloids, free and immobile, present in the fractured rock (see section 4).

Model data requirements include dispersion rates, flow rates, and sorption rates for colloids in fractured rock. Accordingly, such data have been derived, using a mathematical method developed here in the appendix, and its dependence upon colloid size, composition, fracture size, and microscopic surface forces has been analyzed.

The colloid migration analysis in section 2 was based upon theoretical considerations and did not rely on macroscopic, empirically defined constants. We discussed possible validation of the methodology, and the use of the results to make predictions for individual colloid penetration. We obtained the quantitative behaviour of the transport parameters, taking suitable values for the fracture width, groundwater flow rate, and a range of forces due to surface charge. The numerical algorithm used has been verified against analytic results in the special case where surface charges are negligible.

In the subsequent radionuclide-colloid analysis, radionuclides bound to colloids dispersed with the characteristics of their hosts, and the enhancement or retardation of radionuclide migration due to colloidal sorption was assessed. In particular, we automated the calculations of dynamic colloid data and radionuclide breakthrough curves.

The calculated breakthrough curves for radionuclides illustrate the effects of background colloids, see section 4. The radionuclides are present within the fracture either in solution, bound to free colloids or bound to immobile colloid material. Radionuclides may also diffuse into the pore space and become sorbed to the porous rock surfaces.

Clearly it would be desirable to integrate such calculations within the Geosphere cases to be produced for Project 90. By choosing commensurate physical and geochemical parameters the variability of breakthroughs with respect to background levels of colloids could be assessed.

In addition we have discussed the extension of the methodology presented here to cope with spatial and temporal heterogeneities in the distribution of colloids. This included a consideration of the penetration of true colloids, simultaneously dissolving within the fracture groundwater. Such

models, can be made on the basis of the data derived earlier in this report.

We have presented a unified theoretical approach spanning considerations of dispersal and surface forces on the scale of individual colloids $O(10^{-8}\text{m})$, up to the breakthrough behaviour over length scales $O(10^{3}\text{m})$. We feel that a major achievement of this work has been to address the gap between standard continuum migration models, where best-fit parameters are often determined from the available experimental and field data, and the considerations of colloid science, where natural and synthetic colloids and complexes are subject to microscopic analysis.

Appendix: The Asymptotic Spectral Comparison Method

Many transport models for substances in fluid environments contain dispersion terms, designed to model the mixing (or dispersive) phenomena brought about by heterogeneities within the microscopic velocity fields (see [4], [13] and the references therein).

The idea that the velocity varies locally about the mean velocity is illustrated at its simplest by a consideration of Poiseuille (slow) flow through a slab or cylindrical pipe [3].

If our three dimensional pipe-flow model is replaced by a (more computationally amenable) one-dimensional model for transport in the axial direction alone, the inclusion of a dispersion term is, by now, almost standard practice [13].

However, the theoretical basis for such a term is perhaps not so clear, despite intuitive arguments. In particular the original derivation of a dispersive term in this setting relies on no-flux boundary conditions at the pipe walls.

Increasingly scientists are considering fracture-flow problems where idealized fractures allow the outflux of solutes or particles at the walls. The desire to form computationally acceptable models has lead to the continual employment of diffusion-type dispersion terms.

In a recent review of radionuclide transportation by groundwater [12] it was made clear that such hydrodynamic dispersion is a very complex process and the inclusion of Fickian dispersion terms provides only a *simplification of reality.* Moreover, it is often the case that dispersion and molecular diffusion processes are lumped together (since they are qualitatively similar), so that many investigations make it difficult for the reader to appreciate precisely what assumptions are being made, and which processes are being taken into account.

The present interest in dispersal arises from the study of **colloid transport** in groundwater through fractures presented in section 2. Computational requirements force us to simplify the above model to a one-dimensional axial transport problem. Thus one must calculate average advection rates, average capture rates and effective diffusion-dispersion terms for colloids with various properties and sizes.

In this case we shall not simply write down a qualitative *fudge factor*, but rather seek a **theoretical basis** which can be employed in order to reduce

general three-dimensional fracture/pipe-flow problems to one-dimensional axial transport problems.

We shall introduce a general methodology based on an **asymptotic spectral comparison** approach, which seeks to match the spectra of the two problems in a certain asymptotic limit. Then the problems, having a similar spectral behaviour, will show similar time-dependent responses to axial perturbations dominated by low wave numbers. Hence the axial behaviour of the solutions will remain qualitatively and quantitatively similar, and the one-dimensional problem can be realised (in an algebraic sense) as the *best-fit* to the full three-dimensional model.

Taylor's original result [16] is recoverable by the present approach, which is suggestive of its general nature. We shall illustrate these ideas with an example where the classical approach fails to provide any theoretical basis for a Fickian dispersion term.

In this appendix shall concentrate on fracture-flow, and the techniques developed here will be utilized in this report with reference to the colloid transport problems.

We begin by recalling the classical approach to dispersion. The following derivation is due to Sir Geoffrey Taylor [16], [17], and (along with various generalizations [2]) has become an accepted and oft cited basis for the inclusion of an anisotropic Fickian diffusion process as representing dispersal due to local deviations in the advective velocity field.

For brevity we restrict our consideration to the Poiseuille (slow) flow of fluid though a cylindrical pipe of radius L. Let x denote the axial coordinate and r denote the distance from the cylinder axis. Then we consider the transport of some chemical or population of *particles* having concentration or density c. We consider,

$$c_t = D(c_{rr} + \frac{c_r}{r} + c_{xx}) - u_0(1 - \frac{r^2}{L^2})c_x. \tag{31}$$

Here u_0 is constant and $u_0/2$ corresponds to the mean speed of the fluid.

The boundary conditions are

$$c_r = 0 \text{ at } r = L$$

together with the requirement that c be bounded at $r = 0$.

We shall assume that L is small so that cross-fracture diffusion takes place on a more rapid timescale than that associated with longitudinal advection.

Set $z = r/L$ and $y = x - t\theta$, for some constant θ. y provides a moving frame in which to analyse any axial dispersal. Of course we must choose θ appropriately.

Writing c as a function of t, y and z, (31) becomes

$$\frac{L^2}{D}c_t = c_{zz} + \frac{c_z}{z} + L^2 c_{yy} + \frac{L^2}{D}(\theta - u_0(1-z^2))c_y. \tag{32}$$

Now we assume that the $L^2 c_{yy}$ term is negligible, while θ is such that c_t is small (this is equivalent to assuming that the cross-fracture distribution equilibrates rapidly with the source term due to axial advection).

Thus we seek to solve

$$0 = c_{zz} + \frac{c_z}{z} + \frac{L^2}{D}(\theta - u_0(1-z^2))c_y \tag{33}$$

instead of (32) as a first approximation.

Next we make the further assumption that the variation with respect to z in c is small (since the solution is rapidly equilibrated in the z direction). Thus c_y should be thought of as predominantly constant with respect to z, so that we may integrate (33) to obtain

$$c = c_0 - (\theta - u_0)\frac{L^2}{4D}c_y z^2 - u_0 \frac{L^2}{16D}c_y z^4, \tag{34}$$

where c_0 is the value of c at $z = 0$.

Applying the boundary condition at $z = 1$ to (4) we obtain $\theta = u_0/2$, the average flow rate.

Now the total flux, Q, through the cross section y =constant is

$$Q = -2\pi L^2 \int_0^1 c(u_0(1-z^2) - \theta) z \, dz = -\frac{\pi L^4 u_0^2}{192D}c_y. \tag{35}$$

Let $\tilde{c}$ denote the mean concentration over a cross section. Then since our earlier assumptions imply $c \approx \tilde{c}$, we have

$$\pi L^2 \tilde{c}_t + Q_x = 0.$$

Thus

$$\tilde{c}_t = d\tilde{c}_{yy},$$

where

$$d = L^2 u_0^2 / 192D. \tag{36}$$

Hence in (x,t) coordinates we obtain an advection-diffusion equation with dispersion constant given by d.

The limiting factor in this argument is that the no-flux boundary condition cannot be relaxed. We must rely on the fact that $c \approx c_0 \approx \tilde{c}$ across the fracture, and any other boundary condition representing an outflow of particles would result in all these terms being set to zero as a first approximation.

Thus in problems such as the dispersal of species with outflow at the fracture walls, or the dispersal of colloidal particles in fractures, where the colloids sorb to the fracture walls, the above analysis is inappropriate. Moreover in such problems, there is in addition often an advective term across the fracture due to surface forces. Clearly if one dimensional models are to be employed we must set out a new basis for the inclusion and estimation of a Fickian-like dispersal term.

Intuitively, at least the aim is clear. A population of particles, initially located at the same cross-section, will disperse in the axial direction due to the non-uniformity of the velocity field. We wish to *fit* this dispersal to a one dimensional transport model by the imposition of a Fickian diffusion term in the axial direction. Such a term will be referred to as a **dispersion term.**

We have seen how this may be achieved in special circumstances by Taylor's method, but this approach cannot be generalised as it stands. Here we present an alternative approach.

Consider the general advection diffusion model of the form

$$c_t = D(c_{rr} + \frac{c_r}{r} + c_{xx}) - u(r)c_x - \frac{(rv(r)c)_r}{r} \tag{37}$$

together with the boundary condition at $r = L$:

$$\alpha c + \beta c_r = 0,$$

for constants α and β, and the requirement that c be bounded at $r = 0$.

Here $u(r)$ represents the axial advection due to the fluid flow — think of $u(r)$ as $u_0(1 - r^2/L^2)$, while $v(r)$ represents any radial advection due to surface forces, etc.

Equation (37) is linear, so we begin by seeking solutions of the form

$$c = e^{ikx+\sigma t} f(r). \tag{38}$$

We obtain

$$D(f_{rr} + \frac{f_r}{r}) - \frac{1}{r}(rvf)_r - (iku(r) + k^2 + \sigma)f = 0, \tag{39}$$

where

$$\alpha f + \beta f_r = 0 \text{ at } r = L \ ,$$
$$\text{and } f \text{ is bounded at } r = 0.$$

This last problem is an eigenproblem for the pair (σ, f). For each k, fixed, there will be infinitely many solutions $\{(\sigma_m, f_m) : m = 0, 1, 2, \ldots\}$ ordered so that

$$Re(\sigma_0) > Re(\sigma_1) > \ldots$$

Since the corresponding solution u behaves $O(e^{\sigma_m t})$, the zero$^{\text{th}}$ mode will be dominant for all but short times. Let us write $\sigma = \sigma_m(k)$ to express the functional dependence of σ in the m$^{\text{th}}$ mode upon k. Each $\sigma_m(k)$ is a complex valued function of the wave number, k.

The set of values taken by σ as k varies in $\mathbf{R}$, and $m = 0, 1, 2, \ldots$ is known as the **spectrum** for the differential form on the right hand side of (37).

Now consider a one dimensional equation, which we shall use to approximate the axial behaviour of (37);

$$\bar{c}_t = D^* \bar{c}_{xx} - u^* \bar{c}_x - s^* \bar{c}. \tag{40}$$

This incorporates a source/sink term as well as advection and Fickian diffusion. We must choose D^*, u^* and s^* so that

$$\bar{c}(x,t) \approx \frac{2}{a^2} \int_0^a c\, r\, dr \equiv \tilde{c}(x,t),$$

that is, so that the solution of (40), $\bar{c}$, approximates the cross-sectional mean, $\tilde{c}$, of the solution, c, of (37).

Now let us find the spectrum of the differential form on the right hand side of (40). Substituting $\bar{c} = e^{\sigma t + ikx}$ into (40) we obtain

$$\sigma = -D^* k^2 - iku^* - s^*. \tag{41}$$

As k varies, the quadratic (41), usually called the **dispersion curve**, gives the response of the equation (40) to perturbations with wave number, k.

Now integrating rc from (38) with respect to r, and normalizing f, we obtain

$$\tilde{c} = e^{ikx + \sigma t} \ .$$

Recall that the possible relationships between σ and k for the full problem are given by the eigenmodes $\sigma_m(k)$

Now we will have $\tilde{c} \approx \bar{c}$ pro ling the $\sigma - k$ relationship for $\bar{c}$, given by (41), is close to that for $\hat{c}$, which is given by the eigenproblem (39). Of course (39) possesses an extra **degree of freedom** in that one may choose a particular mode (parameterized by integer m). However we have observed that the zeroth mode will dominate for all but short times. Hence in making this **spectral comparison**, we choose D^*, u^* and s^* so that the function

$$\sigma = \sigma_0(k)$$

is approximated by (41). In particular we require that the agreement is good for k small (where $\sigma_0(k)$ is relatively large). Thus an asymptotic approach to the solution of (39) is appropriate.

In summary we proceed as follows.

Firstly we solve (39) asymptotically for small k. It is appropriate to expand σ_0 as a power series. Thus we obtain

$$\sigma_0(k) = \gamma_0 + k\gamma_1 + k^2\gamma_2 + O(k^3) \tag{42}$$

for some constants γ_0, $\gamma_1, \ldots$

Secondly we equate coefficients of successive powers of k between (41) and (42), so that D^*, u^*, and s^* are determined. For these values, the solution of (40) provides an asymptotic approximation to the behaviour of the cross-sectional average of the solution, c, of (37), valid while c is dominated by small wave numbers in the axial direction and by the corresponding simplest eigenmodes in the radial direction.

In fact by using the method of steepest descent [14] one may show that if $\bar{c}(x,0)$ is chosen appropriately, we will have

$$\mid c(x,r,t) - \bar{c}(x,0) f_0(r) \mid \leq O(e^{-s^* t}/t)$$

where f_0 solves (39) when $\sigma = -s^*$ and $k = 0$.

As an illustration of the asymptotic spectral comparison method let us re-examine Taylor's scenario.

Consider the system given by (31). Then in the notation of the previous section we have

$$\frac{D(f_r r)_r}{r} = (\sigma + iku(r) + Dk^2)f \ , \tag{43}$$

where $u(r) = u_0(1 - r^2/L^2)$.

Introducing the asymptotic series

$$\begin{aligned} f &= f_0 + kf_1 + k^2 f_2 + \ldots \\ \sigma &= \gamma_0 + k\gamma_1 + k^2\gamma_2 + \ldots \ , \end{aligned}$$

we substitute for f and σ and solve for successive f_i's, so determining the γ_i's by the imposition of solvability criteria.

To $O(1)$ we obtain

$$D(f_{0_r}r) = r\gamma_0 f_0 \ ,$$
$$f_{0_r} = 0 \text{ at } r = L \ ,$$
$$\text{and } f \text{ bounded at } r = 0.$$

Thus $f_0 \equiv 1$ and $\gamma_0 = 0$.

To $O(k)$, we have

$$D(f_{1_r}r)_r = r(\gamma_1 + iu_0(1 - \frac{r^2}{L^2})) \ ,$$
$$f_{1_r} = 0 \text{ at } r = L \ ,$$
$$\text{and } f_1 \text{ bounded at } r = 0.$$

Integrating both sides from $r = 0$ to $r = L$ we obtain

$$i\gamma_1 = \frac{u_0}{2},$$

the average fluid velocity. For this choice of γ_1 we obtain

$$f_1(r) = \frac{iu_0}{4^2 D}(2r^2 - \frac{r^4}{L^2}) + constant.$$

To $O(k^2)$, we have

$$D(f_{2_r}r)_r = r(\gamma_2 + D + f_1(r)iu_0(\frac{1}{2} - \frac{r^2}{L^2}))$$
$$f_{2_r} = 0 \text{ at } r = L \ ,$$
$$\text{and } f_2 \text{ bounded at } r = 0.$$

Integrating both sides from $r = 0$ to $r = L$ we obtain

$$\begin{aligned} \gamma_2\frac{L^2}{2} + D\frac{L^2}{2} &= \frac{u_0^2}{16D}\int_0^L (2r^2 - \frac{r^4}{L^2})(\frac{1}{2} - \frac{r^2}{L^2})r\,dr \\ &= -\frac{u_0^2 L^4}{D4.96}. \end{aligned}$$

Thus

$$\gamma_2 = -D - \frac{u_0^2 L^2}{D192}.$$

Hence

$$\sigma = -\frac{iku_0}{2} - Dk^2 - \frac{u_0^2 L^2 k^2}{D192} + O(k^3). \tag{44}$$

Comparing (44) with (41) we must choose

$$\begin{aligned} D^* &= D + \frac{L^2 u_0^2}{D.192} \\ u^* &= \frac{u_0}{2} \\ s^* &= 0 \end{aligned}$$

for our one dimensional model (40). The correction

$$\frac{L^2 u_0^2}{D.192}$$

to the axial diffusion term agrees precisely with that given by d in (36). Thus we have recovered Taylor's result.

However the advantage of the present approach is that it remains valid in circumstances where the earlier analysis fails.

Consider the following example of a two dimensional fracture of constant width, $2L$, in the (x, z) plane.

We have;

$$c_t = D(c_{xx} + c_{zz}) - u(z)c_x \quad x \in \mathbf{R},\ z \in (0, L),\ t \geq 0\ , \tag{45}$$

$$c = 0 \quad z = L$$

$$c_x = 0 \quad z = 0.$$

Notice that we are imposing a zero boundary concentration at the fracture wall, which will cause an outflux of particles from the fracture.

In the notation of the previous section, (39) becomes

$$Df_{zz} = (\sigma + iku(z) + k^2 D)f \tag{46}$$

$$f = 0 \quad z = L$$

$$f_x = 0 \quad z = 0.$$

We shall calculate the dispersion curve $\sigma = \sigma_0(k)$ obtained from the simplest mode solutions to (46) and compare it to (41) asymptotically, for small k, just as in the previous example.

Let us first choose

$$u(z) = u_0(1 - \frac{z^2}{L^2})\frac{3}{2} ,$$

so that we again have Poiseuille flow along the fracture.

Substituting

$$\begin{aligned} f &= f_0 + kf_1 + k^2 f_2 + \dots \\ \sigma &= \gamma_0 + k\gamma_1 + k^2\gamma_2 + \dots , \end{aligned}$$

into (46), to $O(1)$ we obtain

$$Df_{0_{zz}} = \gamma_0 f_0$$

$$f = 0 \quad z = L$$

$$f_{0_z} = 0 \quad z = 0.$$

Whose simplest solution is given by

$$f_0 = A\cos(\frac{\pi z}{2L}) \text{ and } \gamma_0 = -\frac{\pi^2 D}{4L^2}.$$

for any constant A. Without loss of generality we take $A = 1$.

To $O(k)$ we obtain

$$f_{1_{zz}} + \frac{\pi^2}{4L^2} f_1 = \frac{(\gamma_1 + iu(z))f_0(z)}{D} -$$

$$f_1 = 0 \quad z = L$$

$$f_{1_z} = 0 \quad z = 0.$$

Multiplying by $\cos(\frac{\pi z}{2L})$, and integrating from $z = 0$ to $z = L$, we obtain

$$\gamma_1 \int_0^L \cos^2(\frac{\pi z}{2L})\, dz = -iu_0 \frac{3}{2} \int_0^L (1 - \frac{z^2}{L^2}) \cos^2(\frac{\pi z}{2L})\, dz.$$

For this value of γ_1 one may calculate

$$f_1 = \frac{2L}{\pi} \left\{ \sin(\frac{\pi z}{2L}) \int_0^z \cos(\frac{\pi s}{2L}) r(s)\, ds - \cos(\frac{\pi z}{2L}) \int_0^z \sin(\frac{\pi s}{2L}) r(s)\, ds \right\} + h\cos(\frac{\pi z}{2L})$$

where $r(z) = (\gamma_1 + iu(z))f_0(z)/D$, and h is any constant.

Notice that

$$\int_0^a \cos(\frac{\pi z}{2L}) r(z)\, dz = 0 ,$$

by definition of γ_1.

Finally, to $O(k^2)$ we have,

$$f_{2zz} + \frac{\pi^2}{4L^2} f_2 = \frac{((\gamma_2 + D) f_0(z) + (\gamma_1 + iu(z)) f_1(z)}{D}$$

$$f_2 = 0 \quad z = L$$

$$f_{2z} = 0 \quad z = 0.$$

Multiplying by $\cos(\frac{\pi s}{2L})$, and integrating from $z = 0$ to $z = L$, we obtain

$$(\gamma_2 + D) \int_0^L \cos^2(\frac{\pi z}{2L})\, dz = -\int_0^L (\gamma_1 + iu(z)) f_1(z) \cos(\frac{\pi z}{2L})\, dz$$

from which we determine γ_2. (The term with the constant h in f_1 makes no contribution to this last integral.)

Thus we have determined

$$\sigma = \gamma_0 + \gamma_1 k + \gamma_2 k^2 + O(k^3)$$

and γ_0, γ_1, and γ_2 determine r, u^*, and D^* (respectively) in (41). In this case a long calculation ensues in order to calculate D^*. We have

$$s^* = \frac{\pi^2 D}{4L^2} \tag{47}$$

$$u^* = (1 + \frac{3}{\pi^2}) u_0 \tag{48}$$

$$D^* = D + \frac{L^2 u_0^2}{D} \frac{0.026303995}{\pi^2}$$

Note also that u_0 is the average axial velocity of the fluid which is less than the average axial velocity, u^*, of the particles, or solute.

It is interesting to compare the above results with the dispersion coefficient arrived at by Taylor's theory (when the zero boundary condition imposed on (45) at $z = L$ is replaced by $c_z = 0$). In this case

$$s^* = 0$$

$$u^* = u_0$$

$$D^* - D = \frac{2u_0^2 L^2}{105 D}$$

In [10] various mathematical models are developed for the migration of colloids in fractured rock. Here we consider such a model where colloids

are subject to advection, by the groundwater flow within the fracture, as well as attractive surface forces between themselves and the fracture walls.

Let a denote the radius of a colloid particle and let $c(x,z,t)$ denote the density of free colloids in a uniform slot fracture (with symmetry in the y-direction). We have

$$c_t = D(a)(c_{xx} + c_{zz}) - u(z)c_x - (v(a)c)_z \tag{49}$$

for

$$x \in \mathbf{R},\ z \in (0, L-a)\ ,$$
$$c_z = 0 \quad z = 0\ ,$$
$$c = 0 \quad z = L - a\ ,$$

(compare (49) with (1)).

Using our asymptotic spectral comparison method, we may calculate the terms D^*, u^*, s^* in (40), so that (40) represents an axial transport process asymptotically equivalent to that for the cross sectional average of c, given by (49). We have performed a number of such numerical calculations in this report (see section 2). Notice that v may be singular at $z = L - a$, so care must be taken there, [10]. The results are comparable to those given in [10], where a slightly different approach was taken. In particular in [10] dispersion is ignored, an assumption vindicated by our present analysis for small colloids, but less useful as a is increased.

The results for u^* and s^* are qualitatively of the form anticipated in [10], but D^* is not monotone decreasing due to the presence of a dispersion term. However this last, $D^* - D$, is not straightforward since a standard Taylor dispersion term could only yield

$$D^* = D + O(\frac{1}{D}) = O(\frac{1}{a}) + O(a)$$

and not the sigmoidal behaviour observed in section 2.

The asymptotic spectral comparison method developed here, as part of this project may well be of wider interest, and it is envisaged that a fuller account of this will be published shortly in a suitable scientific journal.

References

[1] A. Avogadro and G. de Marsily, The role of colloids in nuclear waste disposal, in; Scientific Basis for Nuclear Waste Management, Boston, 1983.

[2] R. Aris, On the dispersion of a solute in a fluid flowing through a tube, *Proc. Roy. Soc.* A. **235**, 67, 1956.

[3] G.K. Batchelor, An Introduction to Fluid Dynamics, Cambridge University Press, London, 1967.

[4] J. Bear, Dynamics of Fluids in Porous Media, Elsevier, Amsterdam, 1972.

[5] J. Dodds, Particle size measurement by hydrodynamic chromatography and field flow fractionation, preprint, CRNS-ENSIC, Nancy.

[6] I.S. Gradshteyn and I.M. Ryzhik, Tables of Integrals, Series, and Products, Corrected and Enlarged Edition, Academic Press, London, 1980.

[7] J. Granger, J. Dodds, D. Leclerc and N. Midoux, Flow and diffusion of particles in a channel with one porous wall: Polarization chromatography, *Chem. Eng. Sci.*, **41**, 3119-3128, 1988.

[8] R. Grauer, Zur chemie von kolloiden: Verfuegbare sorptionsmodelle und zur frage der kolloidhaftung, PSI-Bericht Nr.65, Würenlingen, Mai 1990.

[9] J. Gregory, Interfacial Phenomena, in: Sci. Basis of Filtration, Ed., K.J. Ives, Noordhoff-Leyden, 1975.

[10] P. Grindrod, Colloid-nuclide migration in fractured rock: mathematical model specification, SKI Technical Report TR 89:17, June 1989.

[11] Y. Hwang, T.H. Pigford, W.W.L. Lee and P.L. Chambre, Analytic solution of pseudocolloid migration in fractured rock, LBL-27249, UCB-NE-4158, submitted for the 1989 American Nuclear Society Winter Meeting, June 1989.

[12] D.A. Lever, Radionuclide Transport by Groundwater Flow Through the Geosphere: Current Status, NSS/G105, Harwell Laboratory, UKAEA, 1989.

[13] G. de Marsily, Quantitative Hydrology, Academic Press, London, 1986.

[14] J.D. Murray, Asymptotic Analysis, Springer, Berlin, 1984.

[15] A. Talbot, An accurate numerical inversion of Laplace transforms, *J. Inst. Maths Applics* **23**, pp97-120, 1979.

[16] Sir Geoffrey Taylor, Dispersion of soluble matter in solvent flowing slowly through a tube, *Proc. Roy. Soc.* A. **219**, 186, 1953.

[17] Sir Geoffrey Taylor, The dispersion of matter in turbulent flow through a pipe, *Proc. Roy. Soc.* A. **223**, 446, 1954.

[18] B.J. Travis and H.E. Nuttall, A transport code for radiocolloid migration: with an assessment of an actual low-level waste site, *Mat. Res. Soc. Symp. Proc.*, **44**, 1985.

[19] K.J. Worgan and P.C. Robinson, A one dimensional model of a fractured rock geosphere and its interface with CALIBRE, INTERA-ECL Report I2420-1 DRAFT, 1990.

Index

www.ski.se

STATENS KÄRNKRAFTINSPEKTION
Swedish Nuclear Power Inspectorate

POST/POSTAL ADDRESS SE-106 58 Stockholm
BESÖK/OFFICE Klarabergsviadukten 90
TELEFON/TELEPHONE +46 (0)8 698 84 00
TELEFAX +46 (0)8 661 90 86
E-POST/E-MAIL ski@ski.se
WEBBPLATS/WEB SITE www.ski.se